AIMS Mathematics, 11(11): 39215–39259.
DOI: 10.3934/math.20261510
Received: 21 May 2026
Revised: 07 September 2026
Accepted: 14 September 2026
Published: 24 November 2026

https://www.aimspress.com/journal/Math

*Research article*

# Prey preference as a driver of predator coexistence: a novel two-predator $n$-prey model based on the descriptive statistical index

**Hanan Saeed**[1], **Nouf A. Alrubea**[2], **Mehmet Yavuz**[3,4,5,*] **and Ali Sarrah**[1]

[1] Department of Mathematics, Faculty of Science, Al-Baha University, Alaqiq 65779-7738, Saudi Arabia

[2] Department of Mathematics, College of Science, Jouf University, Sakaka 72441, Saudi Arabia

[3] Department of Mathematics and Computer Sciences, Faculty of Science, Necmettin Erbakan University, Konya 42090, Turkiye

[4] Centre for Environmental Mathematics, University of Exeter, Cornwall TR10 9FE, United Kingdom

[5] Department of Applied Mathematics and Informatics, Kyrgyz-Turkish Manas University, Bishkek 720038, Kyrgyzstan

* **Correspondence:** Email: M.Yavuz@exeter.ac.uk.

**Abstract:** A novel two-predator, $n$-prey model based on an extended Holling type-II functional response that incorporates mutual temporal interference between two different predator species is proposed and analyzed, allowing for both identical and non-identical feeding behaviors. Due to the establishment of positivity and boundedness of all solutions, the model is biologically well-posed. Also, we establish theorems on the global stability of the coexistence state in both symmetric and asymmetric feeding cases, along with their proofs using suitable Lyapunov functions. Moreover, the stability of the axial equilibria is characterized using the reproduction numbers. To quantify predators' specialization (the degree to which predators focus on particular prey over others) on the classes of prey species, a unique preference index is invented via integrating three parameters (attack rate, handling time, and conversion efficiency) into a single metric. Numerical simulations, using a Runge-Kutta method, validate the analytical derivations and demonstrate how predator specialization and prey preference shape long-term competition and survival in multi-species ecosystems. Expectedly, our findings reveal diverse dynamic behaviors including "dichotomous dynamical partitioning", where generalist predatory species show opposing behaviors. In a nutshell, this work uncovers more complex dynamics, such as steady regimes, oscillatory regimes, and various coexistence patterns, in contrast to simpler models already investigated in the existing literature.

**Keywords:** predator-prey interactions; extended Holling type-II; complex dynamics
**Mathematics Subject Classification:** 37N25, 62P10, 92B10

## 1. Introduction

Several mathematical models have been taken into consideration in order to comprehend and analyze the dynamic relationships between prey and predators [1, 2]. A number of researchers have examined their models because they account for several factors such as time delays, harvesting, and the spread of disease among populations [3–5]. They present various interesting dynamics, although different functional responses are used. Undoubtedly, the functional response of the predator, or the quantity of prey ingested by each predator in a given amount of time, is always considered as the primary component of any model studying predator-prey interactions.

Van Leeuwen et al. [6] investigated the generalization of functional response for a predator that alternates between a number of species. In [7], Kar employed Holling type-II to analyze the stability of a prey-predator model that included a prey refuge. The Holling type-II functional response, which is distinguished by a slowing intake rate, is the most advantageous functional response [8]. This kind of functional response was employed by several authors to simulate the dynamics of predator-prey interactions. For instance, the dynamics of a predator-prey model with a Holling type-II functional response were examined by Molla et al. [9]. Also, a predator-$n$-prey model with an extended Holling type-II functional response was developed by Fatah et al. [10] to analyze species interactions.

In reality, many predators feed on multiple kinds of prey. For example, many large land species, including antelopes, buffaloes, pigs, and zebras, are usually preyed upon by lions. Moreover, different predator species repeatedly compete for the same prey resources in some ecosystems. For example, in African savannas, lions and hyenas fight for similar food species, such as wildebeest and zebras. In North American ecosystems, wolves and bears also share prey like elk and deer. From a mathematical point of view, studying such trophic interactions is necessary to understand the complicated ecological dynamics created by the interaction of numerous predator species and multiple prey species.

While several studies have created models with one predator consuming multiple prey species [6, 11], the more ecologically realistic scenario of two predator species competing for multiple prey resources has received considerably less attention, particularly when using the Holling type-II functional response. The inclusion of two predators introduces fundamentally important ecological complexities that are absent in single-predator models. Leading among these is the role of prey preference, where each predator may exhibit differential selectivity for certain prey species based on factors such as prey size, behavior, habitat use, or vulnerability. Such preferences can lead to niche partitioning, potentially reducing direct competition and facilitating coexistence.

When prey preferences overlap significantly, interspecific competition between predators intensifies, resulting in feedback loops that affect not only predator populations but also the entire community structure. The presence of two predators thus supports a rich spectrum of possible dynamical regimes, including stable coexistence through resource partitioning, competitive exclusion of the inferior competitor, or more complex oscillatory behaviors arising from the association between competitive interactions and predation pressure. These dynamics are further complicated by the fact that the functional response type of each predator depends not only on its own handling times and attack rates but also on those of its competitor, as both species share the same prey environment and their foraging activities are mutually interfering in time. Understanding these complex relationships is essential for predicting the fate of two-predator, multi-prey communities in natural ecosystems.

Systematically, this paper analyzes the complex dynamics of a novel model featuring two

temporally interfering predators with prey preferences, using an extended Holling type-II functional response. Section 2 extends the Holling type-II response to $n$-classes of prey interacting with two temporally interfered predator species. Section 3 mathematically formulates the model incorporating this extended response. Section 4 thoroughly proves positivity and boundedness of the model's solutions. Section 5 derives all equilibria based on symmetric and asymmetric predator feeding behaviors, establishing coexistence conditions through ecological reproduction numbers. Sections 6 and 7 present numerical simulations for a six-prey, two-predator case, illustrating rich dynamical regimes. Finally, concluding remarks and future study plans are provided in Section 8.

## 2. Extended Holling type-II functional response for two predators

To extend the Holling-type functional response to two predator species feeding on $n$ distinct prey classes, we consider an ecosystem consisting of $n$ prey classes and two predator species. For each prey class $i = 1, 2, \ldots, n$, let the subscripts 1 and 2 denote predator 1 and predator 2, respectively. We then assume the following:

(1) $X_i(t)$: The population density of the $i$-th prey class at time $t$, assumed uniform across the foraging area and shared by both predator species during the interval $[0, t]$.

(2) $N_{i1}(t)$: The total number of prey of class $i$ that are attacked, captured, and handled (and ultimately consumed) by one individual of predator 1 during the interval $[0, t]$.

(3) $N_{i2}(t)$: The total number of prey of class $i$ that are attacked, captured, and handled (and ultimately consumed) by one individual of predator 2 during the interval $[0, t]$.

(4) $T_{i1}$: The handling time (constant) required for an individual predator 1 to consume one prey of class $i$.

(5) $T_{i2}$: The handling time (constant) required for an individual predator 2 to consume one prey of class $i$.

Following the standard Holling-type derivation, we assume that all attacked prey are eventually consumed, so that the terms "attacked" and "consumed" are used interchangeably in the mathematical formulation. This assumption is a modeling idealization that holds when failed attacks are negligible or when the predator only initiates attacks it can successfully complete.

To derive the formula used in this study of the extended Holling type-II functional response for two predators, we develop the extended functional response for one predator in [10] and follow the classical argument of Holling [8]. We define the total time interval of interest as $[0, t]$, during which we measure the cumulative consumption by the predators. During this interval, each predator divides its time exclusively between searching for prey and handling captured prey, with no other activities consuming time. The choice of 0 as the starting point is without loss of generality because the system is autonomous (time-independent); only the duration $t$ matters for the consumption rates.

Furthermore, we assume that the handling time per prey individual is constant for each predator-prey class combination, denoted by $T_{i1}$ for a single individual of predator 1 and $T_{i2}$ for a single individual of predator 2. The key ecological assumption is that these handling times are additive in the sense that the total handling time of both predators consumes from a shared temporal foraging window. This does

not imply that one predator physically prevents the other from searching; rather, it reflects a shared environmental constraint, such as a limited diel activity period (e.g., both species are nocturnal), a fleeting prey availability occurrence, or a finite tidal window for intertidal foraging. In such scenarios, the total handling time by both predators reduces the time available for searching for each individual predator because both species operate within the same constrained time budget. Thus, if $N_{i1}(t)$ and $N_{i2}(t)$ are the numbers of prey of class $i$ consumed by one individual of predator 1 and predator 2, respectively, during the interval $[0, t]$, then the total handling time over this interval is given by

$$\sum_{j=1}^{n} N_{j1}(t)T_{j1} + \sum_{j=1}^{n} N_{j2}(t)T_{j2}. \tag{2.1}$$

In other words, Eq (2.1) represents the cumulative handling time invested by both predators over the interval $[0, t]$. This cumulative handling time reduces the shared search time available to each predator because both species are subject to the same environmental time constraints (e.g., a limited foraging window or a finite daily activity period). The additivity captures the ecological reality that, within a shared temporal niche, time spent handling prey by one species is time that cannot be used for searching by either species, not due to physical interference, but due to the finite duration of the foraging opportunity.

Through the shared time constraints, the two predator species' foraging activities are indirectly competitive. The total handling time of both species decreases the amount of time available for looking for each species because both species forage at the same interval. This is because both species act normally within the same limited temporal window rather than because of direct interference. So, since the total time in the interval $[0, t]$ is either spent searching or handling, the time available for searching, $T_{\text{search}}(t)$, is mathematically given by the remainder

$$T_{\text{search}(t)} = t - \sum_{j=1}^{n} N_{j1}(t)T_{j1} - \sum_{j=1}^{n} N_{j2}(t)T_{j2}. \tag{2.2}$$

Note that we have defined $N_{j1}(t)$ and $N_{j2}(t)$ as total numbers of prey of class j consumed by one individual of predator 1 and one individual of predator 2 during the entire time interval t, respectively. We also can observe that $T_{search}(t)$ is time-dependent and not a constant value, where it denotes the search time available to one individual of either species (assuming the two different predatory individuals forage during the same time interval). Biologically, Eq (2.2) informs that the total time available to one individual of either species is the same interval of time. During this interval, each individual spends some time handling captured prey and the remaining time searching for new prey. Because both species forage during the same interval, the handling time of one individual of the predator 1 species and the handling time of one individual of the predator 2 species both reduce the search time available to a single individual of either species.

We start with defining $N_{i1}(t)$ as the cumulative number of prey consumed up to time $t$ (i.e., over the interval $[0, t]$). Later, its derivative $\frac{dN_{i1}}{dt}$ will give the instantaneous consumption rate at time $t$, which represents the interested quantity for the predator population dynamics.

As in functional response theory [8], we can assume that the number of prey of class $i$ attacked (and subsequently consumed) by one individual of predator 1 is proportional to the prey density $X_i$ and the time available for searching $T_{\text{search}}$. This proportionality reflects the assumption that encounters

between predator and prey occur randomly, and that every encounter leads to a successful attack that is eventually consummated with a handling time. Thus, this expressed as

$$N_{i1}(t) = \alpha_{i1} X_i(t) T_{search}(t). \tag{2.3}$$

Similarly, the number of prey attacked by the individual of predator 2 from class $i$ is proportional to the prey density $X_i$ and the time available for searching $T_{search}$, which is mathematically given by

$$N_{i2}(t) = \alpha_{i2} X_i(t) T_{search}(t). \tag{2.4}$$

The parameters $\alpha_{i1}$ and $\alpha_{i2}$ are the attack rates of predator 1 and predator 2, respectively, on prey class $i$. The attack rate quantifies the efficiency with which a predator encounters, detects, and successfully captures prey. Mathematically, $\alpha_{i1}$ is the per capita rate of successful attacks per unit prey density per unit search time. Biologically, the attack rate integrates several factors such as the predator's searching speed and how quickly it finds prey, how often encounters lead to successful attacks, and how easily prey are detected. For example, a specialized predator may have a high attack rate on its preferred prey and a low attack rate on non-preferred prey, reflecting behavioral adaptations. Contrary to that, a generalist predator may have moderate attack rates across multiple prey classes. Therefore, it is essential to distinguish the attack rate from the handling time $T_{i1}$ (which measures the time spent processing a captured prey item).

In Eqs (2.3) and (2.4), $\alpha_{i1}$ and $\alpha_{i2}$ are the attack rates for the two individuals of predator 1 and predator 2 on prey class $i$, respectively. Inserting Eq (2.2) in Eqs (2.3) and (2.4) gives

$$N_{i1}(t) = \alpha_{i1} X_i(t) \left( t - \sum_{j=1}^{n} N_{j1}(t) T_{j1} - \sum_{j=1}^{n} N_{j2}(t) T_{j2} \right) \tag{2.5}$$

for the individual of predator 1, and

$$N_{i2}(t) = \alpha_{i2} X_i(t) \left( t - \sum_{j=1}^{n} N_{j1}(t) T_{j1} - \sum_{j=1}^{n} N_{j2}(t) T_{j2} \right) \tag{2.6}$$

for the individual of predator 2. Note that the assumption that all attacked prey are consumed is considered as a standard simplification in the derivation of the Holling type-II functional response. In reality, predators may fail to capture some attacked prey due to escape, defense, refuge, or other factors. However, incorporating failed attacks would require more parameters because of the inclusion of attack success probability and would not change the qualitative saturating shape of the functional response. For this study's objectives, where we only focus on the long-term dynamics of predator-prey communities, this simplification is both standard and justified. Readers interested in exploring biological models with failed attacks are referred to [12].

Accordingly, we do not deny the limitations of the assumption that all attacked prey are consumed because predators may experience failed attacks due to prey escape, anti-predator defenses, or interference from other predators in natural systems. Therefore, our intended model does not explicitly track failed attacks; instead, we implicitly follow the classical Holling framework in which the handling time accounts for the time from attack initiation to consumption completion, and the attack rate $\alpha_{i1}$ (or $\alpha_{i2}$) represents the rate of successful encounters only. This assumption is obviously reasonable

when attack success rates are high or when the model is considered at a rough temporal scale where failed attacks are averaged out. The model can be expanded by adding a separate attack success probability parameter in cases where unsuccessful attacks are common and ecologically significant. Although these extensions are beyond the scope of this study, they establish an important field for further investigation.

Therefore, incorporating the time constraint (Eq (2.2)) helps derive the final consumption rates for the two predatory individuals, which is a a saturating (Holling type-II) function of prey density. Mathematically speaking, differentiating Eqs (2.5) and (2.6), with respect to time, yields

$$\frac{dN_{i1}(t)}{dt} = \alpha_{i1}X_i(t) - \alpha_{i1}X_i(t)\left(\sum_{j=1}^{n}\frac{dN_{j1}(t)}{dt}T_{j1} + \sum_{j=1}^{n}\frac{dN_{j2}(t)}{dt}T_{j2}\right),$$
$$\frac{dN_{i2}(t)}{dt} = \alpha_{i2}X_i(t) - \alpha_{i2}X_i(t)\left(\sum_{j=1}^{n}\frac{dN_{j1}(t)}{dt}T_{j1} + \sum_{j=1}^{n}\frac{dN_{j2}(t)}{dt}T_{j2}\right).$$

To simplify, we temporarily symbolize

$$S(t) = \sum_{j=1}^{n}\frac{dN_{j1}(t)}{dt}T_{j1} + \sum_{j=1}^{n}\frac{dN_{j2}(t)}{dt}T_{j2}.$$

Then, we have

$$\frac{dN_{i1}(t)}{dt} = \alpha_{i1}X_i(t) - \alpha_{i1}X_i(t)S(t), \tag{2.7}$$
$$\frac{dN_{i2}(t)}{dt} = \alpha_{i2}X_i(t) - \alpha_{i2}X_i(t)S(t). \tag{2.8}$$

Multiplying Eq (2.7) by $T_{i1}$ and summing over all $i$, and similarly multiplying Eq (2.8) by $T_{i2}$ and summing over all $i$, we obtain

$$\sum_{i=1}^{n}\frac{dN_{i1}(t)}{dt}T_{i1} = \sum_{i=1}^{n}\alpha_{i1}X_i(t)T_{i1} - S(t)\sum_{i=1}^{n}\alpha_{i1}X_i(t)T_{i1}, \tag{2.9}$$
$$\sum_{i=1}^{n}\frac{dN_{i2}(t)}{dt}T_{i2} = \sum_{i=1}^{n}\alpha_{i2}X_i(t)T_{i2} - S(t)\sum_{i=1}^{n}\alpha_{i2}X_i(t)T_{i2}. \tag{2.10}$$

Adding Eq (2.9) with Eq (2.10) and noting that the sum on the left-hand side equals $S(t)$, we get

$$S(t) = \sum_{i=1}^{n}\alpha_{i1}T_{i1}X_i(t) + \sum_{i=1}^{n}\alpha_{i2}T_{i2}X_i(t) - S(t)\left(\sum_{i=1}^{n}\alpha_{i1}T_{i1}X_i(t) + \sum_{i=1}^{n}\alpha_{i2}T_{i2}X_i(t)\right).$$

Solving for $S(t)$ gives

$$S = \frac{\sum_{i=1}^{n}\alpha_{i1}X_iT_{i1} + \sum_{i=1}^{n}\alpha_{i2}X_iT_{i2}}{1 + \sum_{i=1}^{n}\alpha_{i1}X_iT_{i1} + \sum_{i=1}^{n}\alpha_{i2}X_iT_{i2}},$$

$$S(t) = \frac{\sum_{j=1}^{n}\alpha_{j1}T_{j1}X_j(t) + \sum_{j=1}^{n}\alpha_{j2}T_{j2}X_j(t)}{1 + \sum_{j=1}^{n}\alpha_{j1}T_{j1}X_j(t) + \sum_{j=1}^{n}\alpha_{j2}T_{j2}X_j(t)}.$$

Substituting back into Eqs (2.7) and (2.8), we obtain

$$\frac{dN_{i1}(t)}{dt} = \frac{\alpha_{i1}X_i(t)}{1 + \sum_{j=1}^{n} \alpha_{j1}T_{j1}X_j(t) + \sum_{j=1}^{n} \alpha_{j2}T_{j2}X_j(t)}, \tag{2.11}$$

$$\frac{dN_{i2}(t)}{dt} = \frac{\alpha_{i2}X_i(t)}{1 + \sum_{j=1}^{n} \alpha_{j1}T_{j1}X_j(t) + \sum_{j=1}^{n} \alpha_{j2}T_{j2}X_j(t)}, \tag{2.12}$$

which represent the extended Holling type-II functional response. So, we have mathematically shown that $\frac{dN_{i1}(t)}{dt}$ and $\frac{dN_{i2}(t)}{dt}$ are the final consumption rates of a single individual of predator 1 and a single individual of predator 2, respectively. This means that the total consumption by predator species 1 is obtained by multiplying the per-capita consumption in Eq (2.11) by the population size. Similarly, the total consumption is multiplied by predator species 2.

Both predator species consume prey from the same shared prey area $X_i(t)$. This allows the existence of exploitative competition whereby consumption by one species reduces the prey density available to the other. This shared resource is mathematically captured in $1 + \sum_{j=1}^{n} \alpha_{j1}T_{j1}X_j(t) + \sum_{j=1}^{n} \alpha_{j2}T_{j2}X_j(t)$. This obviously suggests that the consumption by one species reduces the prey density attacked by the other because they share the same prey resource.

We emphasize that the additivity of handling times assumes that both predators share the same temporal foraging constraints. This assumption is biologically realistic when predators are active during the same diel period (for example, both are diurnal or both are nocturnal) or when they forage in the same habitat during the same seasonal window. However, this assumption does not work when predators show spatial separation (foraging in different habitats), temporal separation (active at different times of day), or they are subject to independent time constraints. For such scenarios, the intended model can be generalized by replacing the common denominator with predator-specific denominators, as later presented in model (5.13). This generalization is an ecologically relevant addition of the shared-time approach and enables the model to reflect independent foraging restrictions.

Briefly, our derived extended Holling type-II functional response, mathematically described in Eqs (2.11) and (2.12), is biologically motivated by the well-established saturation effect in predator feeding, where the consumption rate increases with prey availability but eventually levels off due to handling time and other limiting factors. In comparison with the derivation of [10], ours is improved and appropriate for systems involving two predators because it allows the predators' feeding behavior to be described in a way that captures both multiple prey species and interspecific interaction.

The mathematical expressions in Eqs (2.11) and (2.12) represent the instantaneous per capita consumption rates of predator 1 and predator 2, respectively, on prey class $i$ at time $t$. To understand why these are "final" consumption rates, note that $N_{i1}(t)$ in Eqs (2.5) and (2.6) is the cumulative number of prey consumed over the entire interval $[0, t]$. Its derivative $\frac{dN_{i1}}{dt}$ is the rate at which prey are being consumed at the instant $t$. By differentiating and solving them as a system of equations, we get rid of the cumulative quantities $N_{i1}(t)$ and $N_{i2}(t)$, obtaining explicit formulas (2.11) and (2.12) that depend only on the current prey densities $X_i(t)$ and the constant parameters $\alpha_{i1}, T_{i1}, \alpha_{i2}, T_{i2}$. These formulas are hence called the final consumption rates because they are the rates that appear directly in the predator population dynamics equations in model (3.2). For example, the total consumption rate of prey class $i$ by predator species 1 is $\frac{dN_{i1}}{dt} \cdot y_1$.

Similar functional responses, their extensions, and prey preferences by predators have been widely used in ecological modeling and are theoretically and experimentally supported by various studies,

see [6, 10, 11]. Accordingly, the proposed model formulation here gives biological significance for analyzing the dynamics of two predators interacting with multiple prey species in a mathematical manner.

## 3. Model formulation

Based on the extended functional response derived above, we now formulate the complete novel model system. We assume the following:

(A1) Each prey class $X_i$ grows logistically at an intrinsic growth rate $r_i > 0$ and carrying capacity $k_i > 0$ in the absence of the predatory species.

(A2) Predator 1, which is denoted as $Y_1$, consumes prey according to the functional response in Eq (2.11) with conversion efficiency $\theta_{i1}$ (the fraction of consumed prey species converted into predator 1 biomass).

(A3) Predator 2, which is notated as $Y_2$, consumes prey according to the functional response in Eq (2.12) with conversion efficiency $\theta_{i2}$ (the fraction of consumed prey biomass assimilated and converted into predator 2 biomass).

(A4) In the absence of prey, predator 1 and predator 2 species decay exponentially with death rates $d_1 > 0$ and $d_2 > 0$, respectively.

(A5) The biological constraint $0 < \theta_{i\mathcal{Z}} \leq \alpha_{i\mathcal{Z}}$ holds for all $i = 1, \ldots, n$ and $\mathcal{Z} = 1, 2$, reflecting that conversion efficiency cannot exceed the predation rate due to metabolic constraints.

Using the final consumption rates derived in Eqs (2.11) and (2.12), the total consumption of prey class $i$ by predator 1 is $\frac{dN_{i1}}{dt} \cdot Y_1$ and by predator 2 is $\frac{dN_{i2}}{dt} \cdot Y_2$. Substituting the derived formulas (2.11) and (2.12) into the prey and predator equations yields our formulated two-predator, $n$-prey model system

$$\begin{aligned}
\frac{dX_i}{dT} &= r_i X_i \left(1 - \frac{X_i}{k_i}\right) - \frac{\alpha_{i1} X_i Y_1}{1 + \sum_{j=1}^{n} \alpha_{j1} T_{j1} X_j + \sum_{j=1}^{n} \alpha_{j2} T_{j2} X_j} \\
&\quad - \frac{\alpha_{i2} X_i Y_2}{1 + \sum_{j=1}^{n} \alpha_{j1} T_{j1} X_j + \sum_{j=1}^{n} \alpha_{j2} T_{j2} X_j}, \quad i = 1, 2, \ldots, n, \\
\frac{dY_1}{dT} &= \frac{\sum_{j=1}^{n} \theta_{j1} X_j Y_1}{1 + \sum_{j=1}^{n} \alpha_{j1} T_{j1} X_j + \sum_{j=1}^{n} \alpha_{j2} T_{j2} X_j} - d_1 Y_1, \\
\frac{dY_2}{dT} &= \frac{\sum_{j=1}^{n} \theta_{j2} X_j Y_2}{1 + \sum_{j=1}^{n} \alpha_{j1} T_{j1} X_j + \sum_{j=1}^{n} \alpha_{j2} T_{j2} X_j} - d_2 Y_2,
\end{aligned} \tag{3.1}$$

where $X_i(t)$ represents the population biomass (or density) of prey class $i$ at time $t$ for $i = 1, 2, \ldots, n$, while $Y_1(t)$ and $Y_2(t)$ denote the population biomass (or density) of predator species 1 and predator species 2 at time $t$, respectively.

Importantly, we need to clarify how the search time $T_{\text{search}}$ generalizes to our model's dynamics in the two cases examined in this study. For the symmetric predator case (identical predators), a single search time $T_{\text{search}}(t)$ is shared by both species, as handling by either predator reduces the search time of both. The per-capita consumption rates are multiplied by the respective population densities $Y_1(t)$ and $Y_2(t)$, yielding the single-denominator model (see model (3.2)). For the asymmetric predator case (non-identical predators), each species possesses its own search time, with handling by one species not affecting the other's search time. This reflects independent foraging constraints (e.g., spatial or temporal separation) and leads to the two-denominator structure as later explored in model (5.13). In both cases, we deliberately assume that all individuals within each species are identical in their foraging parameters, allowing per-capita rates to be scaled by population biomass.

It is also important to distinguish between the saturation of the functional response and the prey's carrying capacity. The functional response (already derived in Eqs (2.11) and (2.12)) saturates as prey density $X_i$ increases, approaching the maximum consumption rate $\frac{1}{T_{i1}}$, which is only determined by the predator's handling time. This saturation limit is obviously independent of the prey's carrying capacity $k_i$. The carrying capacity affects the equilibrium abundance and prey's growth, but it never determines the predator's maximum feeding rate. So, instead of assuming that saturation occurs at carrying capacity, our developed model permits a range of possible results based on the selected parameter values.

It is worth pointing out that the biological assumptions are primarily mathematical simplifications introduced to make our formulated model analytically tractable. We admit that they may not hold in all natural systems and therefore state these mathematical simplifications as follows:

(S1) We assume that predator reproduction is directly proportional to the biomass of prey consumed, with no density-dependent constraints on predator population growth (e.g., no carrying capacity for predators). To be more specific, when a predator consumes prey biomass, a fraction $\theta_{i1}$ of that biomass is converted into new predator biomass, while the remainder is lost to maintenance. This conversion efficiency $\theta_{i1}$ is captured by the positive growth terms $\sum_{j=1}^{n} \theta_{j1} X_j Y_1$ in the predator equations, which stand for the total biomass of new predators produced from consumed prey. In the complete absence of prey, the predator populations go extinct due to starvation, as captured by the mortality terms $-d_1 Y_1$ and $-d_2 Y_2$. We appreciate that in reality, predator reproduction may be subject to density-dependent constraints (e.g., limited breeding sites or territoriality). However, this simplification is standard in mathematical ecology [13] and allows us to derive analytical expressions for the reproduction number $R_0$ and stability conditions, providing a baseline understanding of the formulated model's dynamics before adding more complexities.

(S2) We mathematically assume that the attack rates $\alpha_{i1}, \alpha_{i2}$ and handling times $T_{i1}, T_{i2}$ are constant parameters. However, these parameters may vary with learning behavior, predator satiation, prey density, or environmental conditions depending on the type of natural system. For instance, prey may develop anti-predator defenses, or predators may become more efficient with experience over time. Treating these parameters as constants is a standard simplification in mathematical ecology [13] that enables us to focus primarily on the qualitative dynamics of our model, such as the conditions for coexistence, stability, and extinction. As our objective is to understand the long-term equilibrium behavior of the formulated model, this assumption provides a clear tractable baseline for mathematical and dynamical analysis. Future extensions could incorporate

parameter variation to scrutinize more complicated ecological scenarios.

(S3) We mathematically assume that the two predators and multiple prey species are mixed in space, which means that trophic interactions depend only on population densities and not on spatial distribution. This is also a simplification commonly used in ordinary differential equation models. Here, we avoid studying spatial heterogeneity in our formulated model as incorporating spatial structure in the model requires partial differential equations, which are beyond the scope of this study.

(S4) We make the assumption that predators do not biologically adjust their foraging strategies in response to changing prey availability. Our developed model (3.1) investigates predator preferences through the preference indices (PFI), which intentionally assign constant attack rates $p_i$ and handling times $b_i$ to each prey class, even though some natural predators may move between prey classes based on their trophic consumption. This simplification gives us a tractable baseline for future extended studies that include adaptive behavior. Plus, it enables us to isolate the effect of variable prey preferences on predator-prey dynamics.

(S5) We here assume to examine two different predatory cases: symmetric and asymmetric. When both predator species share identical parameter sets, model (3.1) reduces to a symmetric version that only isolates the impacts of foraging strategies and prey community structure, namely, the predators have the same preference of prey classes. Conversely, when the predators are assigned non-identical parameter sets, it becomes asymmetric, allowing us to examine how variation in foraging efficiency, prey preferences, and competitive abilities between the predators affects dynamic behavior, coexistence, and the model's stability.

The novel model system (3.1) examines the case whereby $n$-classes of prey species are consumed by two different predator species in the ecosystem, showing that the predation rate for each predator depends not only on its own handling times but also on the handling times of the competing predator species. This mutual temporal interference through shared prey resources is captured mathematically in the common denominator $1+\sum_{j=1}^{n}\alpha_{j1}T_{j1}X_j+\sum_{j=1}^{n}\alpha_{j2}T_{j2}X_j$. As a result, the same denominator appears in all the interaction terms of the model system. This symmetry reflects the ecological reality that both predators share the same prey environment and their foraging activities are mutually interfering in time. Therefore, the denominator acts as a common "resource competition" factor that couples the dynamics of both predators. In the limiting case where one predator goes extinct (say, $y_2 \equiv 0$), model system (3.1) reduces to the single-predator model recently studied by Fatah et al. [10].

Our novel complex model system, presented above, possesses several distinctive features that make it particularly well-suited for investigating prey preference dynamics in two-predator multi-prey communities. First, the predator-specific attack rates $\alpha_{i1}$ and $\alpha_{i2}$ provide a direct mathematical representation of each predator's inherent preference for different classes of prey species, allowing researchers to quantitatively explore scenarios ranging from complete generalists ($\alpha_{i1} \approx \alpha_{i2}$ for all $i$) to extreme specialists ($\alpha_{i1} \gg \alpha_{i2}$ for some prey and vice versa for others). Second, the handling time parameters $T_{j1}$ and $T_{j2}$ capture the ecological reality that predators often process preferred prey more efficiently (shorter handling times) than non-preferred prey, creating a mechanistic link between preference and foraging efficiency. Third, the common denominator structure elegantly incorporates the competitive interference between predators through shared time constraints—when one predator

intensifies foraging on its preferred prey, it reduces the searching time available to its competitor, even if they target different prey species. Fourth, the conversion efficiency parameters $\theta_{j1}$ and $\theta_{j2}$ allow modeling of how prey preference translates into reproductive success, with preferred prey typically yielding higher conversion rates. This comprehensive parameterization enables the model to capture the full spectrum of predator-prey interactions, from niche partitioning that promotes coexistence to intense resource competition that may lead to exclusion, all while maintaining biological realism through the saturating Holling type-II functional response.

However, model system (3.1) contains a large number of parameters ($8n + 2$ parameters), which makes mathematical analysis difficult. To reduce the number of parameters and simplify the analysis, we introduce the following dimensionless variables:

$$t = dT, \quad x_i = \frac{X_i}{k_i}, \quad y_1 = \frac{Y_1}{d}, \quad y_2 = \frac{Y_2}{d},$$

where $d = \min(d_1, d_2)$ and $i = 1, 2, \ldots, n$. Substituting these variables into system (3.1) and applying the chain rule, we obtain

$$\begin{aligned}
\frac{dx_i}{dt} &= a_i x_i(1 - x_i) - \frac{p_{i1} x_i y_1}{D(x)} - \frac{p_{i2} x_i y_2}{D(x)}, \quad i = 1, 2, \ldots, n, \\
\frac{dy_1}{dt} &= \frac{\sum_{j=1}^{n} c_{j1} x_j y_1}{D(x)} - \delta_1 y_1, \\
\frac{dy_2}{dt} &= \frac{\sum_{j=1}^{n} c_{j2} x_j y_2}{D(x)} - \delta_2 y_2,
\end{aligned} \tag{3.2}$$

where

$$D(x) = 1 + \sum_{j=1}^{n} b_{j1} x_j + \sum_{j=1}^{n} b_{j2} x_j,$$

and the dimensionless parameters are defined as

$$\begin{aligned}
&a_i = \frac{r_i}{d}, \quad b_{j1} = \alpha_{j1} T_{j1} k_j, \quad b_{j2} = \alpha_{j2} T_{j2} k_j, \quad p_{i1} = \frac{\alpha_{i1} k_i}{d}, \quad p_{i2} = \frac{\alpha_{i2} k_i}{d}, \\
&c_{j1} = \frac{\theta_{j1} k_j}{d}, \quad c_{j2} = \frac{\theta_{j2} k_j}{d}, \quad \delta_1 = \frac{d_1}{d}, \quad \delta_2 = \frac{d_2}{d},
\end{aligned}$$

where all parameters are positive with the biological constraints $c_{j\mathcal{Z}} < p_{i\mathcal{Z}}$ for $\mathcal{Z} = 1, 2$ and all $i$ and $j$. The initial conditions are given in the positive orthant:

$$x_i(0) \geq 0, \quad y_1(0) \geq 0, \quad y_2(0) \geq 0, \quad i = 1, 2, \ldots, n,$$

with at least one initial condition strictly positive. From now on, we deal only with the variables $t$, $x$, and $y$, which represent the dimensionless time and population densities. Thus, all analysis, results, and figures are expressed in terms of these dimensionless variables. Biologically, the dimensionless parameters are interpreted as follows:

- $a_i$: Growth rate of each class of prey species. Increasing this parameter indicates higher-indexed prey species having progressively faster reproductive rates. In the absence of predators, each class follows logistic growth with carrying capacity.
- $p_{iz}$: Attack rate of predator 1 (or predator 2) on prey class $i$. This parameter determines the effectiveness of predator 1 (or predator 2) in encountering, capturing, and successfully consuming prey of class $i$. Higher values on preferred prey indicate more effective attacks, reflecting behavioral specialization.
- $b_{jz}$: Handling time parameter for the prey. Lower values on preferred prey indicate easier capture and shorter consumption time.
- $c_{jz}$: Conversion efficiency of the class of prey to predator 1 biomass. The condition $c_{j1} < p_{i1}$ for preferred prey ensures realistic energy transfer.
- $\delta_z$: Reducing this parameter indicates a longer lifespan for predators, which supports their persistence.

Note that the dimensionless system (3.2) contains $7n + 2$ parameters, representing a reduction of $n$ parameters from the original system (3.1). This reduction simplifies the mathematical analysis while preserving the essential dynamics of the original model system.

In the next sections, we will analyze the dynamical properties of model system (3.2), including positivity, boundedness, stability of equilibrium points, and conditions for population coexistence.

## 4. Positivity and boundedness of solutions for model system (3.2)

Studying positivity and boundedness of model system (3.2) is essential because it guarantees that population densities remain biologically meaningful (non-negative) and do not grow without realistic ecological limits over time. This section will introduce some theorems and their proofs.

**Theorem 4.1.** All solutions of model system (3.2) with non-negative initial conditions remain non-negative for all $t \geq 0$. Furthermore, if the initial conditions are strictly positive, then the solutions remain strictly positive for all finite time.

*Proof.* The right-hand side of system (3.2) is continuous and has continuous partial derivatives on the space $\mathbb{R}^{n+2}_+$ (except possibly at points where denominators vanish, but $D(x) \geq 1 > 0$ for all $x \in \mathbb{R}^n_+$). Therefore, the system satisfies the Lipschitz condition locally, guaranteeing the existence and uniqueness of solutions for any initial condition in $\mathbb{R}^{n+2}_+$.

For invariance of the coordinate planes, consider any class of prey species $x_i$. On the hyperplane $x_i = 0$, we have $\frac{dx_i}{dt}\Big|_{x_i=0} = 0$. Thus, the vector field is tangent to the hyperplane $x_i = 0$, meaning that trajectories cannot cross this hyperplane. If $x_i(0) = 0$, then $x_i(t) = 0$ for all $t \geq 0$. If $x_i(0) > 0$, then $x_i(t)$ cannot become negative.

For positivity of predator populations, if we consider that $y_1$ is located on the hyperplane $y_1 = 0$, then we have $\frac{dy_1}{dt}\Big|_{y_1=0} = 0$ (similarly, for the second predator, $\frac{dy_2}{dt}\Big|_{y_2=0} = 0$). Thus, the vector field is also tangent to the hyperplanes $y_1 = 0$ and $y_2 = 0$. By the same argument, if $y_1(0) = 0$, then $y_1(t) = 0$ for all $t$; if $y_1(0) > 0$, then $y_1(t) > 0$ for all $t$ (and similarly for $y_2$).

For the initial conditions, in terms of strict positivity, with $x_i(0) > 0$, we can show that $x_i(t) > 0$ for all finite $t$. Suppose, for contradiction, that there exists a finite time $t_1 > 0$ such that $x_i(t_1) = 0$ and

$x_i(t) > 0$ for $0 \le t < t_1$. Then, by continuity, $x_i(t_1) = 0$. However, from the prey differential equation of model system (3.2),

$$\frac{dx_i}{dt} = x_i\left[a_i(1 - x_i) - \frac{p_{i1}y_1}{D(x)} - \frac{p_{i2}y_2}{D(x)}\right].$$

This can be written as $\frac{dx_i}{dt} = x_i f_i(x, y_1, y_2)$, where $f_i$ is bounded on any finite time interval. Then,

$$x_i(t) = x_i(0)\exp\left(\int_0^t f_i(x(s), y_1(s), y_2(s))\,ds\right) > 0 \quad \text{for all } t \ge 0.$$

This explicit representation shows that $x_i(t)$ cannot reach zero in finite time. The same argument applies to $y_1$ and $y_2$ since

$$\frac{dy_1}{dt} = y_1\left(\frac{\sum_{j=1}^n c_{j1}x_j}{D(x)} - \delta_1\right) = y_1 g_1(x),$$
$$\frac{dy_2}{dt} = y_2\left(\frac{\sum_{j=1}^n c_{j2}x_j}{D(x)} - \delta_2\right) = y_2 g_2(x).$$

Thus, all solutions with strictly positive initial conditions remain strictly positive for all finite time.

Now, we introduce the theorem that asserts the boundedness of prey populations with its proof. The subsequent part is dedicated to analyzing the proof of the formulated model's boundedness, but we need to provide the following preliminary lemma.

**Lemma 4.1.** Consider the subsystem describing the dynamics of a single prey species $x_i$ within the larger system (3.2). The differential equation governing $x_i$ is hence given by

$$\frac{dx_i}{dt} = a_i x_i(1 - x_i) - \frac{p_{i1}x_i y_1}{D(x)} - \frac{p_{i2}x_i y_2}{D(x)},$$

where all parameters and variables are non-negative. Since the predation terms are non-negative, we obtain the following differential inequality:

$$\frac{dx_i}{dt} \le a_i x_i(1 - x_i).$$

Let us consider

$$\frac{dx_i}{dt} \le a_i x_i - a_i x_i^2.$$

Dividing by $x_i^2$ (for $x_i > 0$) and letting $u_i = \frac{1}{x_i}$ gives

$$\frac{du_i}{dt} = -\frac{1}{x_i^2}\frac{dx_i}{dt} \ge -a_i u_i + a_i.$$

By solving this differential inequality, we obtain

$$u_i(t) \le 1 + (u_i(0) - 1)e^{-a_i t}.$$

Returning to $x_i$, we have

$$x_i(t) \leq \frac{x_i(0)}{x_i(0) + (1 - x_i(0))e^{-a_i t}} \quad \text{for all } t \geq 0.$$

From this inequality, we deduce that

$$\limsup_{t\to\infty} x_i(t) \leq 1.$$

Moreover, if $x_i(0) \leq 1$, then $x_i(t) \leq 1$ for all $t \geq 0$. If $x_i(0) > 1$, then $x_i(t)$ decreases monotonically until it enters the interval $[0, 1]$. Thus, each prey population is bounded above by $\max\{x_i(0), 1\}$.

**Theorem 4.2.** All solutions of model system (3.2) with non-negative initial conditions are uniformly bounded for all $t \geq 0$.

*Proof.* As a combined boundedness function, let us define the following function:

$$W(t) = \sum_{i=1}^{n} \frac{x_i(t)}{\varepsilon_i} + \frac{y_1(t)}{\mu_1} + \frac{y_2(t)}{\mu_2}, \tag{4.1}$$

where $\varepsilon_i$, $\mu_1$, and $\mu_2$ are positive constants to be chosen appropriately. The time derivative of $W$ along the solutions is given by

$$\begin{aligned}\frac{dW}{dt} = &\sum_{i=1}^{n} \frac{1}{\varepsilon_i}\left[a_i x_i(1 - x_i) - \frac{p_{i1}x_i y_1}{D(x)} - \frac{p_{i2}x_i y_2}{D(x)}\right] \\ &+ \frac{1}{\mu_1}\left[\frac{\sum_{j=1}^{n} c_{j1}x_j y_1}{D(x)} - \delta_1 y_1\right] + \frac{1}{\mu_2}\left[\frac{\sum_{j=1}^{n} c_{j2}x_j y_2}{D(x)} - \delta_2 y_2\right].\end{aligned}$$

By rearranging these terms, we have

$$\frac{dW}{dt} = \sum_{i=1}^{n} \frac{a_i}{\varepsilon_i}x_i - \sum_{i=1}^{n} \frac{a_i}{\varepsilon_i}x_i^2 + \frac{y_1}{D(x)}\left[\sum_{j=1}^{n}\left(\frac{c_{j1}}{\mu_1} - \frac{p_{j1}}{\varepsilon_j}\right)x_j\right] - \frac{\delta_1}{\mu_1}y_1 + \frac{y_2}{D(x)}\left[\sum_{j=1}^{n}\left(\frac{c_{j2}}{\mu_2} - \frac{p_{j2}}{\varepsilon_j}\right)x_j\right] - \frac{\delta_2}{\mu_2}y_2.$$

Now, we choose the constants $\varepsilon_i$, $\mu_1$, and $\mu_2$ such that

$$\frac{c_{j1}}{\mu_1} - \frac{p_{j1}}{\varepsilon_j} \leq 0 \quad \text{for all } j \quad \text{and} \quad \frac{c_{j2}}{\mu_2} - \frac{p_{j2}}{\varepsilon_j} \leq 0 \quad \text{for all } j.$$

This is possible by taking $\varepsilon_j$ sufficiently small or $\mu_1, \mu_2$ sufficiently large. Thus, one can depend on the following convenient choice of the constants:

$$\varepsilon_j = \frac{\min(p_{j1}, p_{j2})}{2}, \quad \mu_1 = \frac{\max_j(c_{j1})}{\min_j(p_{j1}/\varepsilon_j)}, \quad \mu_2 = \frac{\max_j(c_{j2})}{\min_j(p_{j2}/\varepsilon_j)}.$$

With these choices, the terms involving $y_1$ and $y_2$ in the square terms become non-positive, so the inequality relation (4.1) becomes

$$\frac{dW}{dt} \leq \sum_{i=1}^{n} \frac{a_i}{\varepsilon_i}x_i - \sum_{i=1}^{n} \frac{a_i}{\varepsilon_i}x_i^2 - \frac{\delta_1}{\mu_1}y_1 - \frac{\delta_2}{\mu_2}y_2.$$

Importantly, note that for each $i$, we have

$$\frac{a_i}{\varepsilon_i}x_i - \frac{a_i}{\varepsilon_i}x_i^2 = \frac{a_i}{\varepsilon_i}x_i(1-x_i) \leq \frac{a_i}{4\varepsilon_i}.$$

Since the term, including $x(1-x)$, attains its maximum value, we have

$$\frac{dW}{dt} \leq \sum_{i=1}^{n} \frac{a_i}{4\varepsilon_i} - \frac{\delta_1}{\mu_1}y_1 - \frac{\delta_2}{\mu_2}y_2.$$

If we let $\mathcal{H} = \sum_{i=1}^{n} \frac{a_i}{4\varepsilon_i}$, then

$$\frac{dW}{dt} \leq \mathcal{H} - \min\left\{\frac{\delta_1}{\mu_1}, \frac{\delta_2}{\mu_2}\right\}\left(\frac{y_1}{\mu_1} + \frac{y_2}{\mu_2}\right).$$

However, one can note that $\frac{y_1}{\mu_1} + \frac{y_2}{\mu_2} = W - \sum_{i=1}^{n} \frac{x_i}{\varepsilon_i} \geq W - \sum_{i=1}^{n} \frac{1}{\varepsilon_i}$ (since $x_i \leq 1$ from Lemma 4.1). To have the explicit bound for $W$, we take $\eta = \min\left\{\frac{\delta_1}{\mu_1}, \frac{\delta_2}{\mu_2}\right\}$ and $M = \sum_{i=1}^{n} \frac{1}{\varepsilon_i}$. Hence, we get

$$\frac{dW}{dt} \leq \mathcal{H} - \eta(W - M) = (\mathcal{H} + \eta M) - \eta W. \tag{4.2}$$

By solving this differential inequality, we obtain

$$\frac{dW}{dt} + \eta W \leq \mathcal{H} + \eta M.$$

Multiplying by the integrating factor $e^{\eta t}$ gives

$$\frac{d}{dt}\left(We^{\eta t}\right) \leq (\mathcal{H} + \eta M)e^{\eta t}.$$

Integrating from 0 to $t$ produces

$$W(t)e^{\eta t} - W(0) \leq \frac{\mathcal{H} + \eta M}{\eta}(e^{\eta t} - 1).$$

So, this inequality relation can be rewritten as

$$W(t) \leq W(0)e^{-\eta t} + \frac{\mathcal{H} + \eta M}{\eta}(1 - e^{-\eta t}). \tag{4.3}$$

Thus, for all $t \geq 0$, we have

$$W(t) \leq \max\left\{W(0), \frac{\mathcal{H} + \eta M}{\eta}\right\}.$$

Based on the presence of non-negative terms in Eq (4.1), we can say that the boundedness of individual populations is given by

$$\frac{x_i(t)}{\varepsilon_i} \leq W(t) \quad \Rightarrow \quad x_i(t) \leq \varepsilon_i W(t),$$

$$\frac{y_1(t)}{\mu_1} \leq W(t) \quad \Rightarrow \quad y_1(t) \leq \mu_1 W(t),$$
$$\frac{y_2(t)}{\mu_2} \leq W(t) \quad \Rightarrow \quad y_2(t) \leq \mu_2 W(t).$$

Combining with the bound on $W(t)$, we obtain uniform bounds for all populations.

**Theorem 4.3.** If the set

$$\Omega = \left\{(x_1, \ldots, x_n, y_1, y_2) \in \mathbb{R}_+^{n+2} : x_i \leq 1 \text{ for all } i,\ W \leq \frac{\mathcal{H} + \eta M}{\eta}\right\},$$

then this set is positively invariant and attracts all solutions of model system (3.2).

*Proof.* From Lemma 4.1, if $x_i(0) \leq 1$, then $x_i(t) \leq 1$ for all $t$. If $x_i(0) > 1$, then $x_i(t)$ decreases until it enters $[0, 1]$, but may temporarily exceed 1. However, once a dynamic trajectory enters the region where $x_i \leq 1$ for all $i$, it cannot leave because, on the boundary $x_i = 1$, we have

$$\left.\frac{dx_i}{dt}\right|_{x_i=1} = -\left(\frac{p_{i1}\, y_1}{D(x)} + \frac{p_{i2}\, y_2}{D(x)}\right) \leq 0.$$

Thus, $x_i$ cannot increase above 1 once it is at or below 1. For the $W(t)$ function, from the differential inequality (4.2), we have $\frac{dW}{dt} \leq 0$ whenever $W \geq \frac{\mathcal{H}+\eta M}{\eta}$. Therefore, $W$ cannot exceed this bound once it is within it.

To achieve the attracting property, from the bound defined in relation (4.3), we have

$$\limsup_{t\to\infty} W(t) \leq \frac{\mathcal{H} + \eta M}{\eta}.$$

Combined with $\limsup_{t\to\infty} x_i(t) \leq 1$, this shows that all solutions approach $\Omega$ as $t \to \infty$.

**Corollary 4.1.** All solutions of model system (3.2) have ultimate bounds, satisfying

$$\limsup_{t\to\infty} x_i(t) \leq 1, \quad i = 1, 2, \ldots, n,$$
$$\limsup_{t\to\infty} y_1(t) \leq \mu_1 \frac{\mathcal{H} + \eta M}{\eta}, \ \limsup_{t\to\infty} y_2(t) \leq \mu_2 \frac{\mathcal{H} + \eta M}{\eta}.$$

Due to the biological significance, the positivity and boundedness proofs suggest several facts. Positivity ensures that no species goes extinct in finite time, which is biologically realistic as populations approach zero asymptotically but never reach exactly zero in finite time (except if initially zero). If each prey population is bounded above by its carrying capacity (in dimensionless units, $x_i \leq 1$), reflecting the limited resources in the environment, then this informs the boundedness of prey. For the boundedness of predators, predator populations are bounded due to the limited prey availability. The bound $\frac{\mathcal{H}+\eta M}{\eta}$ represents the maximum "weighted total biomass" that the model system can support. As for positively invariant region, the set $\Omega$ represents the ecological perspective of the entire system—once trajectories enter this region, they cannot leave, reflecting the self-regulating nature of the ecosystem.

## 5. The equilibria of the model system and its ecological reproduction numbers

For model system (3.2), the model's dynamic behavior ends up with a constant or oscillatory regime based on initial conditions and equilibrium points. For the latter, they can be found analytically when

$$\begin{aligned}
&a_i x_i(1-x_i) - \frac{p_{i1}x_i y_1}{D(x)} - \frac{p_{i2}x_i y_2}{D(x)} = 0, \quad i = 1, 2, \ldots, n,\\
&\frac{\sum_{j=1}^{n} c_{j1}x_j y_1}{D(x)} - \delta_1 y_1 = 0,\\
&\frac{\sum_{j=1}^{n} c_{j2}x_j y_2}{D(x)} - \delta_2 y_2 = 0.
\end{aligned}$$

For the unique positive coexistence equilibrium $E^* = (x_1^*, x_2^*, \ldots, x_n^*, y_1^*, y_2^*)$, the following equilibrium conditions must be satisfied:

$$a_i(1-x_i^*) = \frac{p_{i1}y_1^*}{D(x^*)} + \frac{p_{i2}y_2^*}{D(x^*)}, \quad i = 1, 2, \ldots, n, \tag{5.1}$$

$$\frac{\sum_{j=1}^{n} c_{j1}x_j^*}{D(x^*)} = \delta_1, \tag{5.2}$$

$$\frac{\sum_{j=1}^{n} c_{j2}x_j^*}{D(x^*)} = \delta_2. \tag{5.3}$$

However, the consumption patterns of the two predators for their preferred prey classes dictate the equilibrium states, thereby governing the model's dynamic behavior. To better highlight the rich dynamics arising from two predators—making this study more impactful and ecologically meaningful—we extend our analysis to two special cases derived from model system (3.2) as follows:

**Case 1: Symmetric predators**

If both predators exhibit identical feeding behavior, i.e., $p_{i1} = p_{i2} = p_i$, $b_{j1} = b_{j2} = b_j$, $c_{j1} = c_{j2} = c_j$, and $\delta_1 = \delta_2 = \delta$, then model system (3.2) simplifies to

$$\begin{aligned}
&\frac{dx_i}{dt} = a_i x_i(1-x_i) - \frac{p_i x_i(y_1+y_2)}{1+2\sum_{j=1}^{n} b_j x_j}, \quad i = 1, 2, \ldots, n,\\
&\frac{dy_1}{dt} = \frac{\sum_{j=1}^{n} c_j x_j y_1}{1+2\sum_{j=1}^{n} b_j x_j} - \delta y_1, \quad \frac{dy_2}{dt} = \frac{\sum_{j=1}^{n} c_j x_j y_2}{1+2\sum_{j=1}^{n} b_j x_j} - \delta y_2.
\end{aligned} \tag{5.4}$$

Hence, the resultant equilibria can be expressed as summarized in Table 1.

**Table 1.** Equilibrium points of the identical predator system.

| Type | Notation | Expression |
|---|---|---|
| Complete predator-free equilibrium | $E_f$ | $(1, 1, \ldots, 1, 0, 0) \in \mathbb{R}^{n+2}$ |
| Single-predator equilibrium | $E_Y^*$ | $(x_1^*, x_2^*, \ldots, x_n^*, Y^*, 0)$ or $(x_1^*, x_2^*, \ldots, x_n^*, 0, Y^*)$, where $Y^*$ is the total predator biomass |
| Coexistence continuum | $\mathcal{E}$ | $\{(x_1^*, \ldots, x_n^*, y_1, y_2) : y_1 + y_2 = Y^*,\ y_1 \geq 0,\ y_2 \geq 0\}$ |

For the predator-free equilibrium $E_f = (1, 1, \ldots, 1, 0, 0)$, the basic reproduction number $\mathcal{R}_0$ determines whether each predator can invade when at least one class of prey species coexist. Therefore, $x_j = 1$ for all $j$ at this equilibrium model system (5.4) has the following unified reproduction number:

$$\mathcal{R}_0 = \frac{\sum_{j=1}^{n} c_j}{\delta\left(1 + 2\sum_{j=1}^{n} b_j\right)}.$$

As the two predators have identical feeding behavior, the reproduction number $\mathcal{R}_0$ is unified, leading either to stability, in which the predators cannot invade when $\mathcal{R}_0 < 1$, or to instability, in which the predators can invade when $\mathcal{R}_0 > 1$.

In terms of biology, both predators occupy the exact same ecological niche—they consume the same classes of prey species with identical attack rates, handling times, and conversion efficiencies. Consequently, total predation pressure on prey is determined by the sum of both predator populations ($Y^* = y_1 + y_2$) as symbolized in Table 1. This indicates that the two identical predators act additively rather than antagonistically. This may violate the competitive exclusion principle, which states that two predatory species cannot coexist stably in the ecosystem.

**Case 2: Asymmetric predators**

If the two predators have different preferences on classes of prey species (i.e., $p_{i1} \neq p_{i2}$, $b_{j1} \neq b_{j2}$, $c_{j1} \neq c_{j2}$, and $\delta_1 \neq \delta_2$), then they have non-identical feeding behavior. In other words, the first predator "$y_1$" specializes on the $m$ prey classes and the second predator "$y_2$" on the remaining $n - m$ classes. Hence, model system (3.2) is given by

$$\frac{dx_i}{dt} = a_i x_i(1 - x_i) - \begin{cases} \dfrac{p_{i1}x_i y_1}{D(x)}, & i = 1, 2, \ldots, m \quad \text{(prey targeted by predator } y_1 \text{ only)}, \\ \dfrac{p_{i2}x_i y_2}{D(x)}, & i = m+1, \ldots, n \quad \text{(prey targeted by predator } y_2 \text{ only)}, \end{cases} \tag{5.5}$$

$$\frac{dy_1}{dt} = \frac{\sum_{j=1}^{m} c_{j1}x_j y_1}{D(x)} - \delta_1 y_1, \tag{5.6}$$

$$\frac{dy_2}{dt} = \frac{\sum_{j=m+1}^{n} c_{j2}x_j y_2}{D(x)} - \delta_2 y_2. \tag{5.7}$$

For simplicity of biological meaning, prey equation (5.5) tells that each predator prefers certain classes of prey than the others as described in Table 2, which informs that predator 1 feeds only on prey 1 to $m$ and predator 2 feeds only on prey $m + 1$ to $n$. Hence, there are four equilibria in the model system (5.5)–(5.7) summarized as seen in Table 3.

**Table 2.** Feeding patterns of specialist predators on many prey classes.

| | Prey classes | | | | | | | |
|---|---|---|---|---|---|---|---|---|
| **Predator species** | **1** | **2** | $\cdots$ | $m$ | $m+1$ | $m+2$ | $\cdots$ | $n$ |
| $y_1$ | ✓ | ✓ | ✓ | ✓ | × | × | × | × |
| $y_2$ | × | × | × | × | ✓ | ✓ | ✓ | ✓ |

Note: ✓ indicates that the predator feeds on that prey class, while × indicates no feeding.

**Table 3.** Non-identical predator system's equilibria of ODE (5.5)–(5.7).

| **Type** | **Notation** | **Expression** |
|---|---|---|
| Complete predator-free equilibrium | $E_f$ | $(1, 1, \ldots, 1, 0, 0) \in \mathbb{R}^{n+2}$ |
| Predator 1 persistence equilibrium | $E_1^*$ | $(x_{11}^*, x_{21}^*, \ldots, x_{n1}^*, y_1^*, 0)$ where $x_{i1}^*$ satisfy predator 1's equilibrium conditions |
| Predator 2 persistence equilibrium | $E_2^*$ | $(x_{12}^*, x_{22}^*, \ldots, x_{n2}^*, 0, y_2^*)$ where $x_{i2}^*$ satisfy predator 2's equilibrium conditions |
| Coexistence equilibrium | $E^*$ | $(x_1^*, x_2^*, \ldots, x_n^*, y_1^*, y_2^*)$ where all components satisfy both predator equations |

To determine the coexistence of all the species, the reproduction numbers for the two predators, at the predator-free equilibrium $E_f$, $x_j = 1$ for all $j$, take the following forms:

$$\mathcal{R}_0^{(1)} = \frac{\sum_{j=1}^{m} c_{j1}}{\delta_1 \left(1 + \sum_{j=1}^{m} b_{j1} + \sum_{j=m+1}^{n} b_{j2}\right)} \quad \text{and} \quad \mathcal{R}_0^{(2)} = \frac{\sum_{j=m+1}^{n} c_{j2}}{\delta_2 \left(1 + \sum_{j=1}^{m} b_{j1} + \sum_{j=m+1}^{n} b_{j2}\right)}.$$

In detail, the two predators have different $\mathcal{R}_0$ values, allowing different scenarios where one predatory species can invade but the other cannot. In other words, the predator-free equilibrium $E_f$ is locally asymptotically stable if and only if $R_0^{(1)} < 1$ and $R_0^{(2)} < 1$. If $R_0^{(1)} > 1$ and $R_0^{(2)} < 1$, then predator 1 can invade while predator 2 goes extinct, leading to the single-predator equilibrium $E_1^*$. Conversely, if $R_0^{(1)} < 1$ and $R_0^{(2)} > 1$, predator 2 invades while predator 1 goes extinct, yielding $E_2^*$. When both $R_0^{(1)} > 1$ and $R_0^{(2)} > 1$, the model may exhibit various dynamic behaviors including the following:

(I) Extinction: Both predators go extinct at the predator-free equilibrium (if stable) when they have no feeding on any class of prey species.

(II) Coexistence: Both predators persist at a stable positive equilibrium if they occupy different ecological niches.

(III) Competitive exclusion: One predator outcompetes the other due to superior feeding efficiency or, higher death rate.

(IV) Oscillatory behavior: Limit cycles or more complex dynamics may arise if interspecific competition is sufficiently strong.

Biologically, niche partitioning can hold on model system (5.5)–(5.7) because of complete specialization where the two predators can stably coexist by utilizing completely different prey species, avoiding direct competition. More precisely, the predator population $y_1$ eats only the prey $x_1, ..., x_m$, while the predator population ($y_2$) feeds only on the other prey classes, namely, $x_{m+1}, ..., x_n$. This occurs when the coexistence equilibrium $E^*$ becomes attractive for all the nearby trajectories. So, we now introduce the relevant theorem with its analytical proof in the next subsection.

### *5.1. Global stability analysis of $E^*$ for the two-predator model system*

Now, we proceed to define and prove the existence of global stability of the equilibrium $E^*$ to show that all the classes of prey populations with the predator populations persist whenever they start from initial densities in the ecosystem.

**Definition 5.1.** Model system (3.2) is said to be *globally stable* about the coexistence equilibrium $E^*$ if, for any initial condition in the positive orthant $\mathbb{R}^{n+2}_+$, the solution converges to $E^*$.

**Theorem 5.1.** The coexistence equilibrium $E^*$ of model system (3.2) is globally asymptotically stable in the positive orthant $\mathbb{R}^{n+2}_+$, if the following conditions hold for all $i = 1, 2, \ldots, n$:

$$\frac{p_{i1}}{c_{j1}} = \frac{p_{i2}}{c_{j2}} = \kappa_i, \tag{C1}$$

$$\frac{c_{j1}}{\delta_1} = \frac{c_{j2}}{\delta_2} = \eta_i, \tag{C2}$$

$$b_{j1} = b_{j2} = b_j, \tag{C3}$$

$$4a_i > \kappa_i^2 \delta_1 \delta_2 D(x^*). \tag{C4}$$

*Proof.* We first construct a Lyapunov function of the form

$$V(x, y_1, y_2) = \sum_{i=1}^{n} \rho_i \left( x_i - x_i^* - x_i^* \ln \frac{x_i}{x_i^*} \right) + \beta_1 \left( y_1 - y_1^* - y_1^* \ln \frac{y_1}{y_1^*} \right) + \beta_2 \left( y_2 - y_2^* - y_2^* \ln \frac{y_2}{y_2^*} \right), \tag{5.8}$$

where $\rho_i, \beta_1$, and $\beta_2$ are positive constants to be determined. By differentiating $V$ along the trajectories of system (3.2), we have

$$\frac{dV}{dt} = \sum_{i=1}^{n} \rho_i \left( 1 - \frac{x_i^*}{x_i} \right) \frac{dx_i}{dt} + \beta_1 \left( 1 - \frac{y_1^*}{y_1} \right) \frac{dy_1}{dt} + \beta_2 \left( 1 - \frac{y_2^*}{y_2} \right) \frac{dy_2}{dt}. \tag{5.9}$$

Substituting Eq (5.9) into the dimensionless equations of our model system gives

$$\begin{aligned} \frac{dV}{dt} = & \sum_{i=1}^{n} \rho_i \left( 1 - \frac{x_i^*}{x_i} \right) \left[ a_i x_i (1 - x_i) - \frac{p_{i1} x_i y_1}{D(x)} - \frac{p_{i2} x_i y_2}{D(x)} \right] + \beta_1 \left( 1 - \frac{y_1^*}{y_1} \right) \left[ \frac{\sum_{j=1}^{n} c_{j1} x_j y_1}{D(x)} - \delta_1 y_1 \right] \\ & + \beta_2 \left( 1 - \frac{y_2^*}{y_2} \right) \left[ \frac{\sum_{j=1}^{n} c_{j2} x_j y_2}{D(x)} - \delta_2 y_2 \right]. \end{aligned}$$

Using the equilibrium conditions (5.1)–(5.3), we can rewrite

$$a_i x_i^* (1 - x_i^*) = \frac{p_{i1} x_i^* y_1^*}{D(x^*)} + \frac{p_{i2} x_i^* y_2^*}{D(x^*)},$$

$$\frac{\sum_{j=1}^{n} c_{j1}x_j^*}{D(x^*)} = \delta_1 \quad \Rightarrow \quad \delta_1 y_1^* = \frac{\sum_{j=1}^{n} c_{j1}x_j^* y_1^*}{D(x^*)},$$
$$\frac{\sum_{j=1}^{n} c_{j2}x_j^*}{D(x^*)} = \delta_2 \quad \Rightarrow \quad \delta_2 y_2^* = \frac{\sum_{j=1}^{n} c_{j2}x_j^* y_2^*}{D(x^*)}.$$

After some algebraic calculations as follows:

$$\begin{aligned}
\frac{dV}{dt} &= \sum_{i=1}^{n} \alpha_i \left(1 - \frac{x_i^*}{x_i}\right)\left[a_i x_i(1 - x_i) - \frac{p_{i1}x_i y_1}{D} - \frac{p_{i2}x_i y_2}{D}\right] \\
&\quad + \beta_1 \left(1 - \frac{y_1^*}{y_1}\right)\left[\frac{\sum_j c_{j1}x_j y_1}{D} - \delta_1 y_1\right] + \beta_2 \left(1 - \frac{y_2^*}{y_2}\right)\left[\frac{\sum_j c_{j2}x_j y_2}{D} - \delta_2 y_2\right] \\
&= \sum_{i=1}^{n} \alpha_i (x_i - x_i^*)\left[a_i(1 - x_i) - \frac{p_{i1}y_1}{D} - \frac{p_{i2}y_2}{D}\right] \\
&\quad + \beta_1 (y_1 - y_1^*)\left[\frac{\sum_j c_{j1}x_j}{D} - \delta_1\right] + \beta_2 (y_2 - y_2^*)\left[\frac{\sum_j c_{j2}x_j}{D} - \delta_2\right] \\
&= \sum_{i=1}^{n} \alpha_i (x_i - x_i^*)\left[a_i(1 - x_i^*) - a_i(x_i - x_i^*) - \frac{p_{i1}y_1^*}{D} - \frac{p_{i1}(y_1 - y_1^*)}{D} - \frac{p_{i2}y_2^*}{D} - \frac{p_{i2}(y_2 - y_2^*)}{D}\right] \\
&\quad + \beta_1 (y_1 - y_1^*)\left[\frac{\sum_j c_{j1}x_j^*}{D} + \frac{\sum_j c_{j1}(x_j - x_j^*)}{D} - \delta_1\right] \\
&\quad + \beta_2 (y_2 - y_2^*)\left[\frac{\sum_j c_{j2}x_j^*}{D} + \frac{\sum_j c_{j2}(x_j - x_j^*)}{D} - \delta_2\right],
\end{aligned}$$

we obtain

$$\begin{aligned}
\frac{dV}{dt} &= -\sum_{i=1}^{n} \rho_i a_i (x_i - x_i^*)^2 - \sum_{i=1}^{n} \frac{\rho_i p_{i1}}{D(x)}(x_i - x_i^*)(y_1 - y_1^*) - \sum_{i=1}^{n} \frac{\rho_i p_{i2}}{D(x)}(x_i - x_i^*)(y_2 - y_2^*) \\
&\quad + \frac{\beta_1}{D(x)} \sum_{j=1}^{n} c_{j1}(x_j - x_j^*)(y_1 - y_1^*) - \frac{\beta_1 \delta_1}{y_1}(y_1 - y_1^*)^2 \\
&\quad + \frac{\beta_2}{D(x)} \sum_{j=1}^{n} c_{j2}(x_j - x_j^*)(y_2 - y_2^*) - \frac{\beta_2 \delta_2}{y_2}(y_2 - y_2^*)^2.
\end{aligned}$$

To simplify, we choose appropriate Lyapunov coefficients

$$\rho_i c_{j1} = \beta_1 p_{i1} \quad \text{for all } i \text{ and } j, \tag{5.10}$$
$$\rho_i c_{j2} = \beta_2 p_{i2} \quad \text{for all } i \text{ and } j. \tag{5.11}$$

Under condition (C1), we can satisfy both Eqs (5.10) and (5.11) by setting

$$\rho_i = \kappa_i \beta_1 = \kappa_i \beta_2 \quad \Rightarrow \quad \beta_1 = \beta_2 = \beta.$$

With these choices, the cross-terms are cancelled, yielding

$$\begin{aligned}\frac{dV}{dt} = &-\sum_{i=1}^{n} \kappa_i \beta a_i (x_i - x_i^*)^2 - \frac{\beta\delta_1}{y_1}(y_1 - y_1^*)^2 - \frac{\beta\delta_2}{y_2}(y_2 - y_2^*)^2 \\ &+ \sum_{i=1}^{n} \frac{\beta}{D(x)} \left[ c_{i1}(x_i - x_i^*)(y_1 - y_1^*) + c_{i2}(x_i - x_i^*)(y_2 - y_2^*) \right. \\ &\left. - \kappa_i p_{i1}(x_i - x_i^*)(y_1 - y_1^*) - \kappa_i p_{i2}(x_i - x_i^*)(y_2 - y_2^*) \right].\end{aligned}$$

Thus, the terms in the summation vanish identically due to our coefficient choices, giving

$$\frac{dV}{dt} = -\sum_{i=1}^{n} \kappa_i \beta a_i (x_i - x_i^*)^2 - \frac{\beta\delta_1}{y_1}(y_1 - y_1^*)^2 - \frac{\beta\delta_2}{y_2}(y_2 - y_2^*)^2. \tag{5.12}$$

Under condition (C3), where $b_{j1} = b_{j2} = b_j$, we have $D(x) = 1 + \sum_{j=1}^{n} 2b_j x_j$. However, the analytical expression (5.12) no longer contains $D(x)$ explicitly due to our coefficient choices. This simplification obviously relies on the fact that the functional response denominators are identical for both predators. From Eq (5.12), we observe that

$$\frac{dV}{dt} \leq 0 \quad \text{for all } (x, y_1, y_2) \in \mathbb{R}_+^{n+2}$$

with equality if and only if $x_i = x_i^*$ for all $i$, $y_1 = y_1^*$, and $y_2 = y_2^*$. The terms $-\frac{\beta\delta_1}{y_1}(y_1 - y_1^*)^2$ and $-\frac{\beta\delta_2}{y_2}(y_2 - y_2^*)^2$ are clearly non-positive since $\beta, \delta_1, \delta_2 > 0$ and $y_1, y_2 > 0$.

If we let $S = \{(x, y_1, y_2) \in \mathbb{R}_+^{n+2} : \frac{dV}{dt} = 0\}$, then $S$ consists of points where $x_i = x_i^*$ for all $i$, $y_1 = y_1^*$, and $y_2 = y_2^*$. Thus, $S = \{E^*\}$. By LaSalle's invariance principle, every solution starting in $\mathbb{R}_+^{n+2}$ approaches the largest invariant set in $S$, which is simply $E^*$. Therefore, $E^*$ is globally asymptotically stable.

**Remark 5.1.** If the two predators are identical in their feeding behavior, i.e., $p_{i1} = p_{i2} = p_i$, $c_{j1} = c_{j2} = c_j$, $b_{j1} = b_{j2} = b_j$, and $\delta_1 = \delta_2 = \delta$, then conditions (C1)–(C3) are automatically satisfied with $\kappa_i = p_i/c_j$ and $\eta_i = c_j/\delta$. In this case, the coexistence equilibrium $E^*$ reduces to $\mathcal{E}$ (i.e., $y_1^* = y_2^* = y^*/2$), and global stability holds under condition (C4).

From biological perspectives, the conditions required for global stability of the identical predators have the following biological meanings:

- Condition (C1) implies that the ratio of the predation rate to conversion efficiency is the same for both predators on each prey species. This means that the two predators have identical metabolic efficiencies—the benefit ratio of consuming prey $i$ is the same for both predators.
- Condition (C2) implies that the ratio of conversion efficiency to the death rate is the same for both predators. This means that the lifetime reproduction from consuming prey $i$ is identical for both predators.
- Condition (C3) implies that both predators have identical handling times for each prey species. This means they are equally efficient at processing and consuming prey.

- Condition (C4) ensures that prey growth rates are sufficiently high relative to predation pressure to prevent oscillatory behavior.

These conditions essentially require that the two predators are ecologically equivalent in terms of their per-capita effects on the prey and their demographic parameters. When these conditions hold, the two-predator model system behaves like a single-predator system with combined predator biomass, and global stability can be established as shown earlier. However, we next state and prove the case that the two predators have non-identical behavior.

Intuitively, one may believe that the global stability proof for non-identical predators will require stronger conditions than the identical predator case due to the following several reasons:

(1) The denominators of the extended functional response will be different. In other words, $D_1(x) \neq D_2(x)$ certainly introduces additional cross-terms that would be harder to get completely cancelled.

(2) Some coefficients will be constrained. More precisely, the Lyapunov coefficients must satisfy $\rho_i = \frac{\beta_1}{\kappa_i^{(1)}} = \frac{\beta_2}{\kappa_i^{(2)}}$, which requires consistency between the two predators' parameters.

(3) A condition must be added to ensure that prey growth rates are sufficient enough to overcome the destabilizing effects of cross-terms.

Starting from the formulation of the non-identical predator model system (5.5)–(5.7), we need to reformulate it to be as the following system of ordinary differential equations:

$$\begin{aligned} \frac{dx_i}{dt} &= a_i x_i(1-x_i) - \frac{p_{i1}x_i y_1}{D_1(x)} - \frac{p_{i2}x_i y_2}{D_2(x)}, \quad i = 1, 2, \ldots, n, \\ \frac{dy_1}{dt} &= \frac{\sum_{j=1}^{n} c_{j1}x_j y_1}{D_1(x)} - \delta_1 y_1, \\ \frac{dy_2}{dt} &= \frac{\sum_{j=1}^{n} c_{j2}x_j y_2}{D_2(x)} - \delta_2 y_2, \end{aligned} \tag{5.13}$$

where

$$D_1(x) = 1 + \sum_{j=1}^{n} b_{j1}x_j, \quad D_2(x) = 1 + \sum_{j=1}^{n} b_{j2}x_j.$$

It is worth pointing out that model system (5.13) is not algebraically equivalent to model system (3.2). However, it represents an intentional and ecologically significant generalization. In model system (3.2), the single denominator $D(x)$ contains a complicated structure. By contrast, model system (5.13) assumes that the two predators feed on prey under independent foraging constraints, so that the extended functional response of predator $y_1$ ($y_2$) depends only on its own handling terms $b_{j1}$ ($b_{j2}$) via $D_1(x)$ ($D_2(x)$). This mathematical reformulation is ecologically justified when the two predators exhibit temporal niche partitioning. Such scenarios are common in many multi-predator systems [14]. Thus, the original model system (3.2) is considered as a special case of system (5.13). In details, if we set $b_{j1} = b_{j2} = b_j$ for all $j$, then $D_1(x) = D_2(x) = D(x)$, and model system (5.13)

collapses exactly to model system (3.2). This means that the assumptions of the original model are only generalized by the reformulation given above, allowing us to isolate the dynamical effects of prey selection and predator-specific handling without the influence of mutual physical interference.

In addition, the purpose of this reformulation is to make the next proof easier by putting the system in a format that makes it simpler to use Lyapunov-based arguments and demonstrate the coexistence equilibrium's global stability.

**Theorem 5.2.** The coexistence equilibrium $E^*$ of model system (5.13) with non-identical predators is globally asymptotically stable in the positive orthant $\mathbb{R}^{n+2}_+$, if the following sufficient conditions hold for all $i, j = 1, 2, \ldots, n$:

$$\frac{p_{i1}}{c_{j1}} = \kappa_i^{(1)}, \quad \frac{p_{i2}}{c_{j2}} = \kappa_i^{(2)} \quad \text{(proportionality conditions)}, \tag{M1}$$

$$\frac{\delta_1}{c_{j1}} = \frac{\delta_2}{c_{j2}} = \mu, \tag{M2}$$

$$\frac{b_{j1}}{p_{j1}} = \frac{b_{j2}}{p_{j2}} = \tau_j, \tag{M3}$$

$$4a_i > \left( \sqrt{\kappa_i^{(1)}\delta_1} + \sqrt{\kappa_i^{(2)}\delta_2} \right)^2 D_{\max}(x^*) \quad \text{(sufficient prey growth)}, \tag{M4}$$

where $D_{\max}(x) = \max\{D_1(x), D_2(x)\}$.

*Proof.* By constructing the same candidate Lyapunov function mentioned in Eq (5.8) with the same determined positive constants, and then differentiating, we obtain Eq (5.9). Inserting this into the equations of system (5.13), we have

$$\begin{aligned}\frac{dV}{dt} = &\sum_{i=1}^{n} \rho_i \left(1 - \frac{x_i^*}{x_i}\right)\left[a_i x_i(1 - x_i) - \frac{p_{i1}x_i y_1}{D_1(x)} - \frac{p_{i2}x_i y_2}{D_2(x)}\right] \\ &+ \beta_1 \left(1 - \frac{y_1^*}{y_1}\right)\left[\frac{\sum_{j=1}^n c_{j1}x_j y_1}{D_1(x)} - \delta_1 y_1\right] + \beta_2 \left(1 - \frac{y_2^*}{y_2}\right)\left[\frac{\sum_{j=1}^n c_{j2}x_j y_2}{D_2(x)} - \delta_2 y_2\right].\end{aligned}$$

Under the assumption of the following equilibrium conditions at the coexistence equilibrium $E^*$, we have

$$\begin{aligned} a_i x_i^*(1 - x_i^*) &= \frac{p_{i1}x_i^* y_1^*}{D_1(x^*)} + \frac{p_{i2}x_i^* y_2^*}{D_2(x^*)}, \\ \frac{\sum_{j=1}^n c_{j1}x_j^*}{D_1(x^*)} = \delta_1 \quad &\Rightarrow \quad \delta_1 y_1^* = \frac{\sum_{j=1}^n c_{j1}x_j^* y_1^*}{D_1(x^*)}, \\ \frac{\sum_{j=1}^n c_{j2}x_j^*}{D_2(x^*)} = \delta_2 \quad &\Rightarrow \quad \delta_2 y_2^* = \frac{\sum_{j=1}^n c_{j2}x_j^* y_2^*}{D_2(x^*)}. \end{aligned}$$

Using the proportionality conditions (M1), we choose

$$\rho_i p_{i1} = \beta_1 c_{i1} \quad \text{and} \quad \rho_i p_{i2} = \beta_2 c_{i2} \quad \text{for all } i. \tag{5.14}$$

From condition (M1), we have $p_{i1} = \kappa_i^{(1)} c_{j1}$ and $p_{i2} = \kappa_i^{(2)} c_{j2}$. Substituting into relation (5.14) gives

$$\begin{aligned} \rho_i \kappa_i^{(1)} c_{j1} = \beta_1 c_{i1} \quad &\Rightarrow \quad \rho_i \kappa_i^{(1)} = \beta_1 \quad \text{for all } i, \\ \rho_i \kappa_i^{(2)} c_{j2} = \beta_2 c_{i2} \quad &\Rightarrow \quad \rho_i \kappa_i^{(2)} = \beta_2 \quad \text{for all } i. \end{aligned}$$

Thus, $\rho_i = \frac{\beta_1}{\kappa_i^{(1)}} = \frac{\beta_2}{\kappa_i^{(2)}}$, which requires $\frac{\beta_1}{\kappa_i^{(1)}} = \frac{\beta_2}{\kappa_i^{(2)}}$ for all $i$. This is possible if $\frac{\kappa_i^{(1)}}{\kappa_i^{(2)}}$ is constant across $i$, which is implied by the consistency of conditions (M1) and (M2).

By doing some calculations and using the equilibrium conditions for simplifying $\frac{dV}{dt}$, we obtain

$$\begin{aligned} \frac{dV}{dt} = &- \sum_{i=1}^{n} \rho_i a_i (x_i - x_i^*)^2 - \frac{\beta_1 \delta_1}{y_1} (y_1 - y_1^*)^2 - \frac{\beta_2 \delta_2}{y_2} (y_2 - y_2^*)^2 \\ &+ \sum_{i=1}^{n} \frac{\rho_i p_{i1}}{D_1(x)} (x_i - x_i^*)(y_1 - y_1^*) + \sum_{i=1}^{n} \frac{\rho_i p_{i2}}{D_2(x)} (x_i - x_i^*)(y_2 - y_2^*) \\ &- \frac{\beta_1}{D_1(x)} \sum_{j=1}^{n} c_{j1} (x_j - x_j^*)(y_1 - y_1^*) - \frac{\beta_2}{D_2(x)} \sum_{j=1}^{n} c_{j2} (x_j - x_j^*)(y_2 - y_2^*). \end{aligned}$$

Due to our coefficient choices (5.14), the terms involving $D_1(x)$ and $D_2(x)$ combine, but since $D_1(x) \neq D_2(x)$, they cannot be removed completely. Instead, we have

$$\begin{aligned} \frac{dV}{dt} = &- \sum_{i=1}^{n} \rho_i a_i (x_i - x_i^*)^2 - \frac{\beta_1 \delta_1}{y_1} (y_1 - y_1^*)^2 - \frac{\beta_2 \delta_2}{y_2} (y_2 - y_2^*)^2 \\ &+ \sum_{i=1}^{n} \rho_i p_{i1} \left( \frac{1}{D_1(x)} - \frac{1}{D_2(x)} \right) (x_i - x_i^*)(y_1 - y_1^*) \\ &+ \sum_{i=1}^{n} \rho_i p_{i2} \left( \frac{1}{D_2(x)} - \frac{1}{D_1(x)} \right) (x_i - x_i^*)(y_2 - y_2^*). \end{aligned}$$

As condition (M3) implies a relationship between $D_1(x)$ and $D_2(x)$, we assume that

$$\Delta(x) = \left| \frac{1}{D_1(x)} - \frac{1}{D_2(x)} \right| \leq \frac{|D_2(x) - D_1(x)|}{D_{\min}(x)^2},$$

where $D_{\min}(x) = \min\{D_1(x), D_2(x)\}$. Using condition (M3), we can bound $|D_2(x) - D_1(x)| \leq \sum_{j=1}^{n} |p_{j1} - p_{j2}| \tau_j x_j$. We apply inequality estimates for using the inequality $2uv \leq \varepsilon u^2 + \frac{1}{\varepsilon} v^2$ for any $\varepsilon > 0$, we bound the cross-terms:

$$\left| \rho_i p_{i1} \left( \frac{1}{D_1(x)} - \frac{1}{D_2(x)} \right) (x_i - x_i^*)(y_1 - y_1^*) \right| \leq \frac{\rho_i p_{i1} \Delta(x)}{2} \left[ \varepsilon_i (x_i - x_i^*)^2 + \frac{1}{\varepsilon_i} (y_1 - y_1^*)^2 \right].$$

Similarly, for the $y_2$ terms, choosing $\varepsilon_i$ appropriately and using condition (M2) to relate $\delta_1$ and $\delta_2$ to $c_{j1}$ and $c_{j2}$, we obtain

$$\frac{dV}{dt} \leq - \sum_{i=1}^{n} \left[ \rho_i a_i - \frac{\rho_i p_{i1} \Delta(x) \varepsilon_i}{2} - \frac{\rho_i p_{i2} \Delta(x) \epsilon_i}{2} \right] (x_i - x_i^*)^2$$

$$-\left[\frac{\beta_1\delta_1}{y_1}-\sum_{i=1}^{n}\frac{\rho_i p_{i1}\Delta(x)}{2\varepsilon_i}\right](y_1-y_1^*)^2-\left[\frac{\beta_2\delta_2}{y_2}-\sum_{i=1}^{n}\frac{\rho_i p_{i2}\Delta(x)}{2\varepsilon_i'}\right](y_2-y_2^*)^2.$$

From condition (M4), we have $4a_i > \left(\sqrt{\kappa_i^{(1)}\delta_1}+\sqrt{\kappa_i^{(2)}\delta_2}\right)^2 D_{\max}(x^*)$. By continuity, there exists a neighborhood of $E^*$ where a similar inequality holds with $D_{\max}(x)$ replacing $D_{\max}(x^*)$. This ensures that we can choose $\varepsilon_i, \varepsilon_i'$ such that all coefficients in Eq (5.12) are positive. Moreover, using $\rho_i = \frac{\beta_1}{\kappa_i^{(1)}} = \frac{\beta_2}{\kappa_i^{(2)}}$ and condition (M2), we can show that

$$\frac{\beta_1\delta_1}{y_1} > \sum_{i=1}^{n}\frac{\rho_i p_{i1}\Delta(x)}{2\varepsilon_i} \quad \text{and} \quad \frac{\beta_2\delta_2}{y_2} > \sum_{i=1}^{n}\frac{\rho_i p_{i2}\Delta(x)}{2\varepsilon_i'}$$

for appropriately chosen $\varepsilon_i, \epsilon_i$. Therefore, $\frac{dV}{dt} \leq 0$ for all $(x, y_1, y_2) \in \mathbb{R}_+^{n+2}$, with equality only at $E^*$. Thus, if we assume $S = \{(x, y_1, y_2) \in \mathbb{R}_+^{n+2} : \frac{dV}{dt} = 0\}$, $\frac{dV}{dt} = 0$ implies $x_i = x_i^*$ for all $i$, $y_1 = y_1^*$, and $y_2 = y_2^*$. This leads to $S = \{E^*\}$. By LaSalle's invariance principle, every solution starting in $\mathbb{R}_+^{n+2}$ approaches the largest invariant set in $S$, which is simply $E^*$. Hence, the coexistence equilibrium $E^*$ is globally asymptotically stable.

From a biological standpoint, the following biological implications result from the conditions necessary for the non-identical predators' global stability:

- Condition (M1): Attack rates are proportional to conversion efficiencies for each predator-prey pair.
- Condition (M2): Predator death rates scale with conversion efficiencies in a consistent way across both predators.
- Condition (M3): Handling time per unit attack rate is the same for both predators, ensuring a relationship between the denominators.
- Condition (M4): Prey growth must be sufficiently large to overcome the combined predation pressure from both predators.

These conditions, while more restrictive than the identical predator case, are biologically plausible and ensure the global stability of the coexistence equilibrium $E^*$ in our reformulated model system (3.2) with non-identical predators.

## 6. Simulations of nonlinear dynamics and discussions

The formulated model was proved to be well-posed, with all solutions remaining non-negative for positive initial conditions. We established uniform boundedness of solutions through the construction of a suitable function $W(t)$ in Eq (4.1) and demonstrated the existence of a positively invariant attracting region $\Omega$ in $\mathbb{R}_+^{n+2}$. These properties ensure that the novel complex model is biologically realistic, with populations remaining finite and non-negative for all time.

Due to the predators' preference while feeding on the classes of prey species, we have examined two systems: identical and non-identical predators. For validation and confirmation of the consistency of our derived analytical results including the local and global stability of all the equilibria, we solve

both systems numerically for the case $n = 6$ (six classes of prey species) and two predators using the Runge-Kutta method.

We can obviously note that the two studied model systems have three key behavioral and ecological parameters controlled by the prey preference consumed by the two predators, namely, $p_{ij}$, $c_{ij}$, and $b_{ij}$. To integrate them, we provide a single numerical value that captures how strongly a predator prefers each prey species by defining the preference index

$$PFI_{ij} = \frac{p_{ij}\, c_{ij}}{b_{ij}}.$$

Thus, instead of analyzing three separate parameters simultaneously, the PFI condenses them into one interpretable metric. It is effective in our study because it compares scenarios, predators, and prey, provides patterns of specialization and feeding preferences, predicts ecological effects and predator persistence, illustrates complex relationships in time series plots, correlates to stability analysis, and eventually determines the model's parameterization choices by combining three parameters into a single interpretable index. Therefore, the PFI enables us to capture the essential dynamics that reflect the biological significance of the two model systems; without it, we would be confused with a vast array of $p_{ij}, b_{ij}$, and $c_{ij}$ values.

Based on this framework, the two predators have different parameters (preference indices) as depicted in Figure 1, creating distinct biological interactions to cover a wide range of dynamic behaviors for the two systems. As a result, Figure 2 and Figure 3 show how the predatory and prey species interact, providing four meaningful identical and four non-identical scenarios as selected in Table 4 and Table 5, respectively.

### *6.1. Dynamics of the identical predator model system*

To systematically evaluate how predator foraging strategies influence prey dynamics and predator persistence of the identical-predator model system, four distinct ecological scenarios (I1–I4) are parameterized in Table 4, each characterized by a unique distribution of the PFI, which integrates the attack rate ($p_i$), handling time ($b_i$), and conversion efficiency ($c_i$) to quantify the relative predatory pressure exerted on each prey class.

In scenario I1, both predators are identical low-efficiency generalists, characterized by moderate attack rates ($b_i = 0.50$ across all prey classes), low conversion efficiencies ($c_i = 0.25$), and uniform preference indices (PFI = 0.125). The computed reproduction number is $\mathcal{R}_0 = 0.50$, which is significantly below the persistence threshold of 1. This indicates that, under deterministic dynamics, each predator population cannot sustain itself even when preying across all six prey classes. The low conversion efficiency ($c_i = 0.25$) limits the energy gained from each prey encounter, while the moderate attack rate ($b_i = 0.50$) fails to compensate. Consequently, predator biomass declines toward extinction regardless of initial conditions. Prey populations, growing at rates $a_i = 5.0$ to 7.5, experience only weak top-down control and converge to their carrying capacity-limited equilibria. Neither predator can establish a single-predator equilibrium ($E_Y^*$), nor can they coexist. Thus, scenario I1 represents a predator-driven extinction regime where generalist foraging without efficiency leads to community collapse of the predator guild, leaving prey populations released from predation.

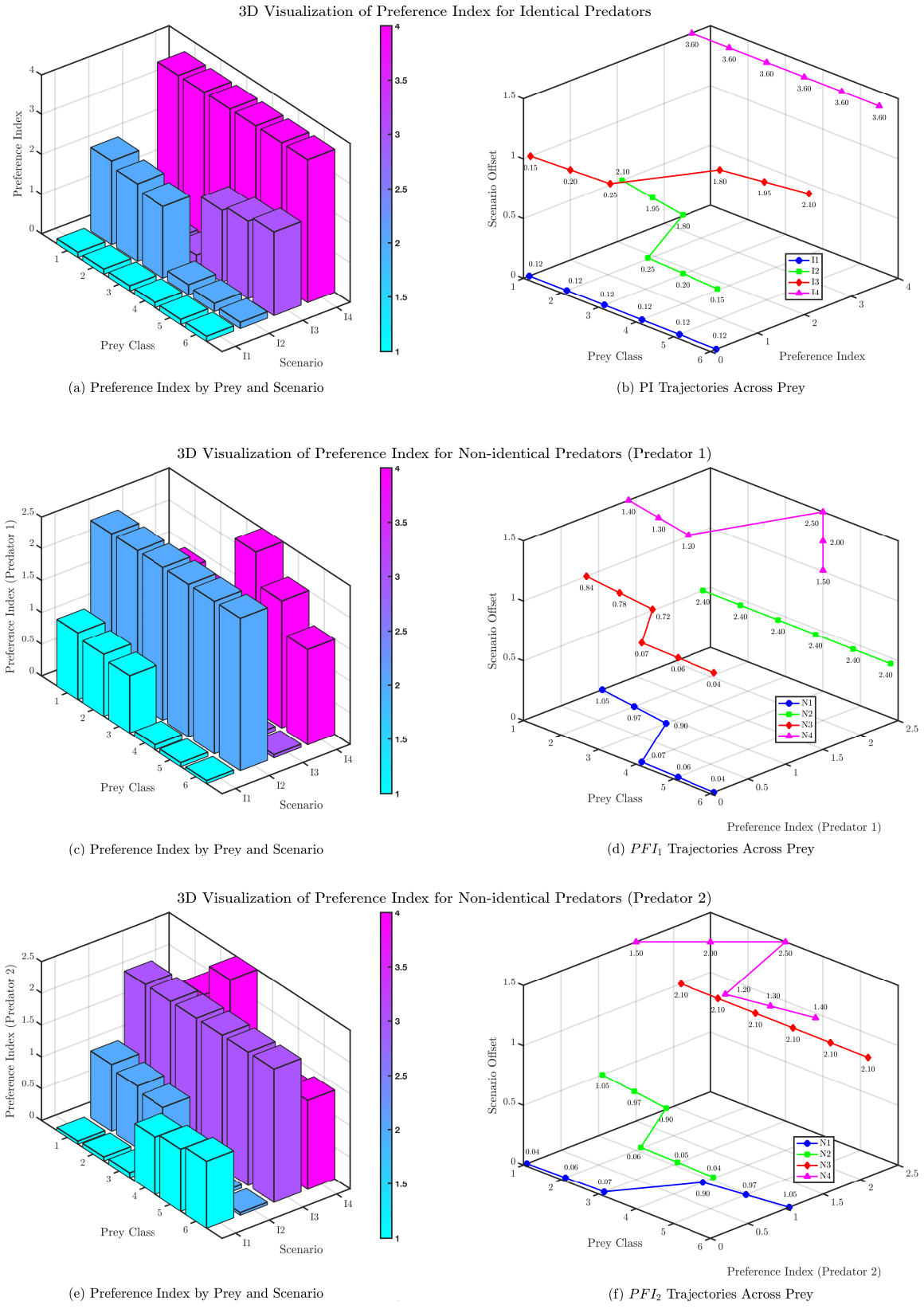


(a) Preference Index by Prey and Scenario

(b) PI Trajectories Across Prey

(c) Preference Index by Prey and Scenario

(d) $PFI_1$ Trajectories Across Prey

(e) Preference Index by Prey and Scenario

(f) $PFI_2$ Trajectories Across Prey

**Figure 1.** Visualization of the preference indices used in this work to study the nonlinear dynamics of identical and non-identical predator systems.

**Table 4.** Four scenarios for identical predators, reflecting the dynamic behaviors simulated in Figure 2, based on the PFI.

| Scenario | Prey Class | Growth Rates $a_i$ | Identical parameters for both predators | | | | Preference Index (PFI) | Reproduction Number |
|---|---|---|---|---|---|---|---|---|
| | | | $p_i$ | $b_i$ | $c_i$ | $\delta$ | | $R_0$ |
| **I1: Low Efficiency Generalists** | 1 | 5.0 | 0.25 | 0.50 | 0.25 | 0.50 | 0.125 | 0.43 |
| | 2 | 5.5 | 0.25 | 0.50 | 0.25 | | 0.125 | |
| | 3 | 6.0 | 0.25 | 0.50 | 0.25 | | 0.125 | |
| | 4 | 6.5 | 0.25 | 0.50 | 0.25 | | 0.125 | |
| | 5 | 7.0 | 0.25 | 0.50 | 0.25 | | 0.125 | |
| | 6 | 7.5 | 0.25 | 0.50 | 0.25 | | 0.125 | |
| **I2: Predatory Specialists (Prefer 1–3)** | 1 | 5.0 | 0.70 | 0.25 | 0.75 | 0.50 | 2.10 | 1.50 |
| | 2 | 5.5 | 0.65 | 0.25 | 0.75 | | 1.95 | |
| | 3 | 6.0 | 0.60 | 0.25 | 0.75 | | 1.80 | |
| | 4 | 6.5 | 0.25 | 0.25 | 0.25 | | 0.25 | |
| | 5 | 7.0 | 0.20 | 0.25 | 0.25 | | 0.20 | |
| | 6 | 7.5 | 0.15 | 0.25 | 0.25 | | 0.15 | |
| **I3: Predatory Specialists (Prefer 4–6)** | 1 | 5.0 | 0.15 | 0.25 | 0.25 | 0.50 | 0.15 | 1.50 |
| | 2 | 5.5 | 0.20 | 0.25 | 0.25 | | 0.20 | |
| | 3 | 6.0 | 0.25 | 0.25 | 0.25 | | 0.25 | |
| | 4 | 6.5 | 0.60 | 0.25 | 0.75 | | 1.80 | |
| | 5 | 7.0 | 0.65 | 0.25 | 0.75 | | 1.95 | |
| | 6 | 7.5 | 0.70 | 0.25 | 0.75 | | 2.10 | |
| **I4: High Efficiency Generalists** | 1 | 5.0 | 1.00 | 0.25 | 0.90 | 0.50 | 3.60 | 2.70 |
| | 2 | 5.5 | 1.00 | 0.25 | 0.90 | | 3.60 | |
| | 3 | 6.0 | 1.00 | 0.25 | 0.90 | | 3.60 | |
| | 4 | 6.5 | 1.00 | 0.25 | 0.90 | | 3.60 | |
| | 5 | 7.0 | 1.00 | 0.25 | 0.90 | | 3.60 | |
| | 6 | 7.5 | 1.00 | 0.25 | 0.90 | | 3.60 | |

**Note:** In all scenarios, we assume that $p_{i1} = p_{i2} = p_i$, $b_{i1} = b_{i2} = b_i$, $c_{i1} = c_{i2} = c_i$, and $\delta_1 = \delta_2 = \delta$, while the preference index is defined as PFI = $\frac{p_i c_i}{b_i}$.

Based on the provided table, scenario I2 is designed as a "predatory specialist" scenario, where predator 1 preferentially targets prey classes 1, 2, and 3 (the lower-growth-rate prey). This is reflected in the parameter assignments: For prey 1–3, the attack rate ($p_i$) is high (0.70, 0.65, 0.60, respectively), while for prey 4–6, the attack rate is low (0.25, 0.20, 0.15). The handling time parameter ($b_i$) is held constant at 0.25 across all prey, and the conversion efficiency ($c_i$) is high (0.75) for the preferred prey and low (0.25) for the non-preferred prey. The PFI, defined as $\frac{p_i \times c_i}{b_i}$, measures overall predatory preference and profitability. In scenario I2, PFI values for prey 1–3 are markedly high (2.10, 1.95, 1.80), while prey 4–6 have very low PFI values (0.25, 0.20, 0.15). This asymmetric preference structure ensures that predator 1 persists by concentrating its foraging on the highly preferred prey 1–3, obtaining sufficient energy intake despite their slower growth rates. Conversely, prey 4–6 experience low predator consumption, meaning they are not heavily targeted by predator 1.

In contrast, scenario I3 reverses the preference pattern: predator 2 preferentially targets prey classes 4, 5, and 6 (the higher-growth-rate prey). Here, for prey 4–6, the attack rate is high (0.60, 0.65, 0.70) with high conversion efficiency (0.75), yielding high PFI values (1.80, 1.95, 2.10), while prey 1–3 receive low attack rates (0.15, 0.20, 0.25) and low PFI values (0.15, 0.20, 0.25). Thus, predator 2 persists by exploiting the faster-growing prey classes 4–6, which can sustain higher predation pressure. Prey 1–3 in this scenario also experience low predator consumption due to the reduced attack rates. The PFI therefore serves as a useful composite metric that captures how the attack rate, handling time, and conversion efficiency jointly determine predator persistence: High PFI values for a predator's preferred prey classes directly support its long-term survival in a multi-prey, multi-predator system.

In scenario I4, both predators have high conversion efficiencies ($c_{i1} = c_{i2} = 0.9$ for all prey classes). This represents a situation where both predators efficiently convert consumed prey biomass into offspring. Consequently, both predator populations can establish and persist. However, due to competition for shared prey resources and the nonlinear nature of the extended Holling type-II functional response, the system exhibits oscillatory dynamics rather than settling to a stable equilibrium. This behavior numerically confirms the analytical derivation of condition (C4). Therefore, this scenario corresponds to the coexistence regime, which represents the most complex and ecologically interesting scenario, where both predators coexist but with non-equilibrium dynamics. This scenario is likely to be common in natural systems where multiple predators share prey resources and all have reasonably efficient conversion of prey biomass into offspring.

Dynamically, the coexistence continuum equilibrium $\mathcal{E}$ takes a place in the system with two identical predators, which means that both predator species can persist together at a balance point, but this balance is not interpreted as a single isolated equilibrium point; instead, it lies along a continuum of possible coexistence states as simulated. This here happens because neither predator has an advantage over the other, so the model system does not select one unique coexistence point. As a result, the populations move toward oscillatory dynamics around that coexistence regime.

In short, the four scenarios, in Figure 2, indicate that the system exhibits different dynamic regimes depending on the preference index. The results show that extinction of both predators occurs due to their competition when the two predators act as low-efficiency generalists. Interestingly, when the predators feed on all prey classes as high-efficiency generalists, the identical predator system shifts to oscillatory dynamics around the coexistence equilibrium.

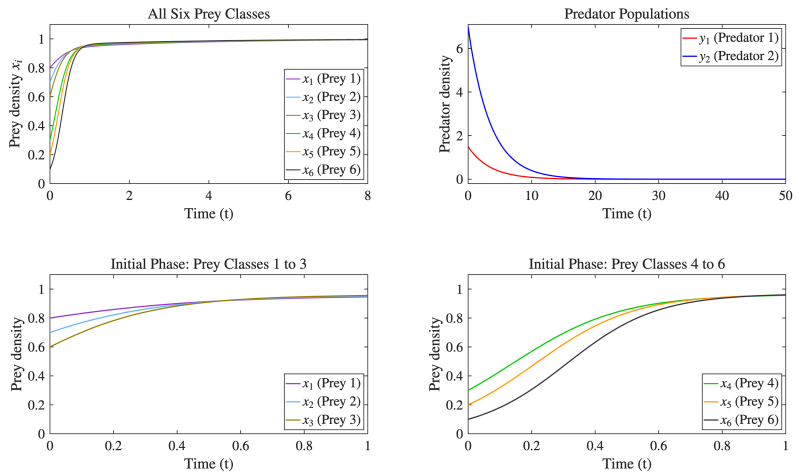


(a) Scenario I1

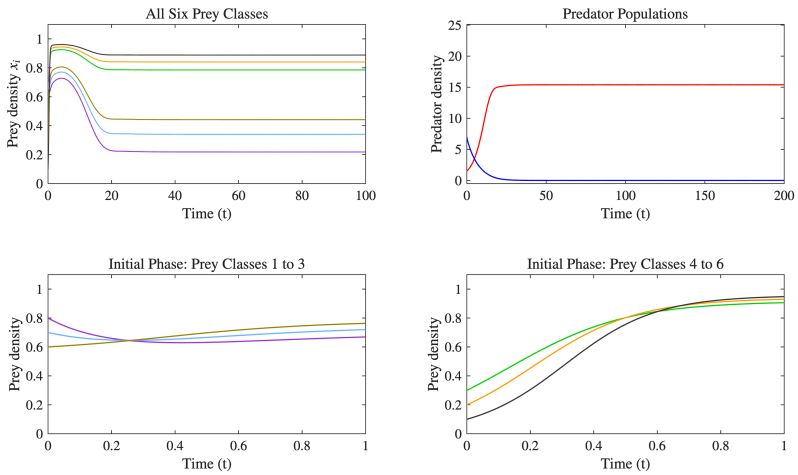


(b) Scenario I2

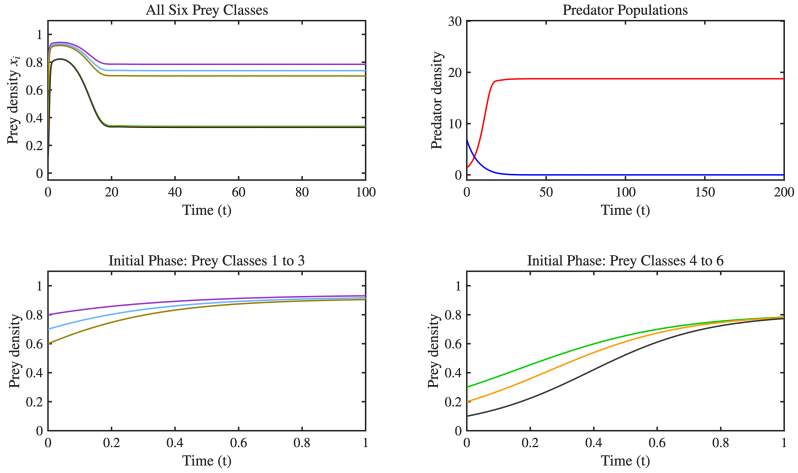


(c) Scenario I3

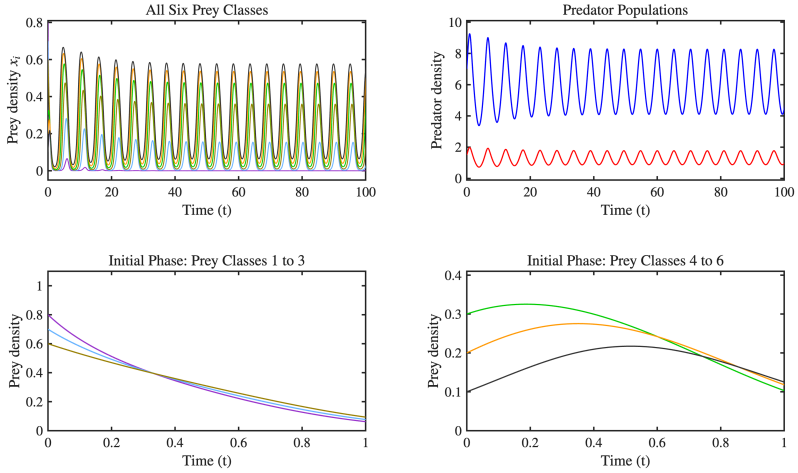


(d) Scenario I4

**Figure 2.** Summary of the four dynamical regimes for the two-predator, six-prey system based on the ecological reproduction numbers $R_{01}$ and $R_{02}$. The results are: (a) Scenario I1: both predators become extinct ($R_{01}, R_{02} < 1$); (b) Scenario I2: only predator 1 becomes extinct ($R_{01} < 1,\ R_{02} > 1$); (c) Scenario I3: only predator 2 becomes extinct ($R_{01} > 1,\ R_{02} < 1$); and (d) Scenario I4: both predators persist ($R_{01}, R_{02} > 1$).

**Table 5.** Four scenarios for non-identical predators, reflecting the dynamic behaviors simulated in Figure 4, based on $PFI_j$.

| Scenario | Prey Class | Growth Rates $a_i$ | Non-identical Parameters for Two Predators | | | | | | | Preference Index | | Reproduction Numbers | |
|---|---|---|---|---|---|---|---|---|---|---|---|---|---|
| | | | $p_{i1}$ | $b_{i1}$ | $c_{i1}$ | $p_{i2}$ | $b_{i2}$ | $c_{i2}$ | $\delta_j$ | $PFI_1$ | $PFI_2$ | $R_0^{(1)}$ | $R_0^{(2)}$ |
| **N1: Complete Niche Partitioning** | 1 | 5.0 | 0.70 | 0.40 | 0.60 | 0.15 | 1.00 | 0.30 | 0.50 | 0.11 | 0.05 | 0.57 | 0.57 |
| | 2 | 5.5 | 0.65 | 0.40 | 0.60 | 0.20 | 1.00 | 0.30 | 0.50 | 0.98 | 0.06 | | |
| | 3 | 6.0 | 0.60 | 0.40 | 0.60 | 0.25 | 1.00 | 0.30 | 0.50 | 0.90 | 0.08 | | |
| | 4 | 6.5 | 0.25 | 1.00 | 0.30 | 0.60 | 0.40 | 0.60 | 0.50 | 0.08 | 0.90 | | |
| | 5 | 7.0 | 0.20 | 1.00 | 0.30 | 0.65 | 0.40 | 0.60 | 0.50 | 0.06 | 0.98 | | |
| | 6 | 7.5 | 0.15 | 1.00 | 0.30 | 0.70 | 0.40 | 0.60 | 0.50 | 0.05 | 0.11 | | |
| **N2: Generalist versus Specialist** | 1 | 5.0 | 0.90 | 0.30 | 0.80 | 0.70 | 0.40 | 0.60 | 0.50 | 2.40 | 1.05 | 1.263 | 0.71 |
| | 2 | 5.5 | 0.90 | 0.30 | 0.80 | 0.65 | 0.40 | 0.60 | 0.50 | 2.40 | 0.98 | | |
| | 3 | 6.0 | 0.90 | 0.30 | 0.80 | 0.60 | 0.40 | 0.60 | 0.50 | 2.40 | 0.90 | | |
| | 4 | 6.5 | 0.90 | 0.30 | 0.80 | 0.25 | 1.20 | 0.30 | 0.50 | 2.40 | 0.63 | | |
| | 5 | 7.0 | 0.90 | 0.30 | 0.80 | 0.20 | 1.20 | 0.30 | 0.50 | 2.40 | 0.05 | | |
| | 6 | 7.5 | 0.90 | 0.30 | 0.80 | 0.15 | 1.20 | 0.30 | 0.50 | 2.40 | 0.04 | | |
| **N3: Specialist versus Generalist** | 1 | 5.0 | 0.70 | 0.50 | 0.60 | 0.90 | 0.30 | 0.70 | 0.50 | 0.84 | 2.10 | 0.74 | 1.15 |
| | 2 | 5.5 | 0.65 | 0.50 | 0.60 | 0.90 | 0.30 | 0.70 | 0.50 | 0.78 | 2.10 | | |
| | 3 | 6.0 | 0.60 | 0.50 | 0.60 | 0.90 | 0.30 | 0.70 | 0.50 | 0.72 | 2.10 | | |
| | 4 | 6.5 | 0.25 | 1.00 | 0.30 | 0.90 | 0.30 | 0.70 | 0.50 | 0.08 | 2.10 | | |
| | 5 | 7.0 | 0.20 | 1.00 | 0.30 | 0.90 | 0.30 | 0.70 | 0.50 | 0.06 | 2.10 | | |
| | 6 | 7.5 | 0.15 | 1.00 | 0.30 | 0.90 | 0.30 | 0.70 | 0.50 | 0.05 | 2.10 | | |
| **N4: Cross Specialization** | 1 | 5.0 | 0.70 | 0.50 | 1.00 | 0.15 | 0.10 | 1.00 | 0.50 | 1.40 | 1.50 | 2.61 | 2.61 |
| | 2 | 5.5 | 0.65 | 0.50 | 1.00 | 0.20 | 0.10 | 1.00 | 0.50 | 1.30 | 2.00 | | |
| | 3 | 6.0 | 0.60 | 0.50 | 1.00 | 0.25 | 0.10 | 1.00 | 0.50 | 1.20 | 2.50 | | |
| | 4 | 6.5 | 0.25 | 0.10 | 1.00 | 0.60 | 0.50 | 1.00 | 0.50 | 2.50 | 1.20 | | |
| | 5 | 7.0 | 0.20 | 0.10 | 1.00 | 0.65 | 0.50 | 1.00 | 0.50 | 2.00 | 1.30 | | |
| | 6 | 7.5 | 0.15 | 0.10 | 1.00 | 0.70 | 0.50 | 1.00 | 0.50 | 1.50 | 1.40 | | |

**Note:** All scenarios maintain the same prey growth rates and predator death rates for consistent comparison between the identical and non-identical predator model systems.

### 6.2. Dynamics of the non-identical predator model system

It is worth pointing out that the chosen parameter set, in Table 5, embodies the principle of niche partitioning through differential prey specialization. Each predator has a clear set of preferred prey where it excels, and no $n$-preferred prey where it performs poorly. This specifically reduces direct competition between the two predators $y_1$ and $y_2$—they are not competing intensely for the same prey classes because each of the two predators prefers certain classes. Instead, they have largely separate trophic resource bases without overlap. This niche partitioning is key to exploring the biological significance of the model system involving two nonidentical predators. In comparison with the model system involving two identical predators, it shows two species competing for identical prey classes as earlier discussed. By giving each predator its own set of preferred prey, we have various nonlinear dynamics including extinction and persistence in steady and oscillatory behaviors.

Covering all the resultant dynamics of the non-identical predator model system can be possible by showing the four scenarios presented in Figure 4, which offers a comprehensive overview, ranging from steady permanent coexistence and oscillatory permanent coexistence to exclusion, for analyzing non-identical predator dynamics. To avoid redundance, we biologically focus on interpreting two scenarios: complete niche partitioning (N1) and generalist predator 1 versus specialist predator 2 (N2).

In scenario N1, the chosen parameterization reflects a strict division of prey resources: predator 1 ($y_1(t)$) exhibits high attack rates ($p_{i1} = 0.70, 0.65, 0.60$) and moderate handling times ($b_{i1} = 0.40$) with conversion efficiency $c_{i1} = 0.60$ for prey classes 1–3, but very low attack rates ($p_{i1} = 0.25, 0.20, 0.15$) and high handling times ($b_{i1} = 1.00$) with low conversion efficiency ($c_{i1} = 0.30$) for prey 4–6. Conversely, predator 2 ($y_2(t)$) informs the opposite pattern: low preference for prey 1–3 ($p_{i2} = 0.15, 0.20, 0.25$; $b_{i2} = 1.00$; $c_{i2} = 0.30$) and high preference for prey 4–6 ($p_{i2} = 0.60, 0.65, 0.70$; $b_{i2} = 0.40$; $c_{i2} = 0.60$).

Biologically, the resulting preference index values, computed as $PFI_1$ and $PFI_2$, obviously reflect this partitioning. For predator 1, $PFI_1$ values are high for prey 1–3 (approximately 1.05, 0.98, 0.90) and very low for prey 4–6 (0.08, 0.06, 0.05). For predator 2, the opposite holds where $PFI_2$ values are low for prey 1–3 (0.05, 0.06, 0.08) and high for prey 4–6 (0.90, 0.98, 1.05). Despite this seemingly efficient niche separation, both reproduction numbers fall below unity ($\mathcal{R}_0 < 1$). This indicates that even though each predator strongly prefers a distinct subset of prey, the magnitude of the PFI values (none exceeding unity) is insufficient to overcome the combined mortality rate ($\delta = 0.50$) and the total handling time burden from all prey in the denominator of the $\mathcal{R}_0$ expression. In other words, the preference indices reveal that while prey selection is highly specialized, the overall profitability of the preferred prey, when integrated across the full suite of prey handled by the two predators, does not produce enough net energy intake to sustain predator populations. Consequently, both predators go extinct, and all six prey populations grow logistically to their carrying capacity.

In scenario N2, the asymmetric foraging strategies yield markedly different preference indices for the two predators. The first predator $y_1(t)$ illustrates uniformly high PFI values ($PFI_1 = 2.40$) across all six prey classes, reflecting its generalist strategy with consistently high attack rates and conversion efficiencies balanced by low handling, the second predator shows a steep gradient in PFI values: relatively higher PFI values for prey 1–3 (1.05, 0.98, 0.90) but dramatically lower values for prey 4–6 (0.63, 0.05, 0.04), indicating a specialist strategy for the second predator $y_2(t)$ that becomes increasingly ineffective against faster-growing prey. This contrast in PFI frameworks directly translates into the reproduction numbers, with $R_{01} > 1$ and $R_{02} < 1$. Therefore, the first predator successfully

invades the prey, but its invasion is characterized by oscillatory behavior rather than a monotonic approach to the equilibrium $E_1^*$. The high and uniform PFI values for the first predator produce sufficiently strong prey consumption across all classes to sustain its population above the extinction threshold, yet the resulting predator–prey interactions create sustained oscillations. Meanwhile, the second predator, despite moderate PFI values on prey 1–3, cannot achieve $\mathcal{R}_0 > 1$ due to its extremely low PFI values on prey 4–6, which collectively fail to provide adequate energy intake when integrated across the full prey spectrum. Thus, only the first consumer persists periodically, driving oscillatory dynamics in the system as seen in Figure 4.

### *6.3. Influence of variations of death rates of the two predators*

Earlier, the selected values of the death rate are set at $\delta_1 = \delta_2 = 0.5$ for the two predators to cover all the possible solutions including free predators regime, free predator 1 regime, free predator 2 regime, and coexistence regime. This configuration satisfies the permanence conditions when appropriate prey lower bounds are established, leading to either steady or oscillatory dynamics depending on the strength of interspecific competition through prey classes. However, examining the influence of varying the two predators' death rates in the two model systems plays a significant role in determining the resultant dynamics because it shows how predator mortality reshapes extinction, persistence, coexistence, and stability in our complex model systems. A change in death rates can switch the feeding behaviors from coexistence to extinction, alter which predator dominates, and shift the balance among prey species. To emulate, we dynamically depict regimes, induced by varying the death rates ($\delta_1$ and $\delta_2$) of the two predators, as four colored regions, where each color informs the behavior as depicted in Figure 3. Due to the competitive exclusion principle, dynamic regimes of Figure 5 show that the single-predator regime prevails in two different regions: red and green.

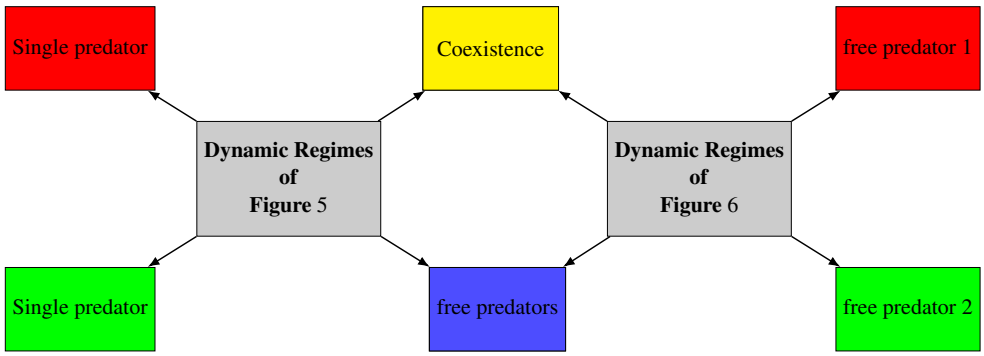


**Figure 3.** Colored regions in the main regime plots indicate the long-term behavior of the two predators: red corresponds to extinction, green to extinction $y_2$, blue to extinction $y_1$, and yellow to coexistence.

To understand how predator mortality reshapes coexistence, dominance, and extinction outcomes in the system. In particular, changing these parameters reveals transitions between different dynamical behaviors and highlights the sensitivity of the 2-predator, 6-prey model to mortality-driven perturbations. The color-coded panels make these regime shifts visually clear by separating the parameter ranges associated with distinct attractors and stability patterns.

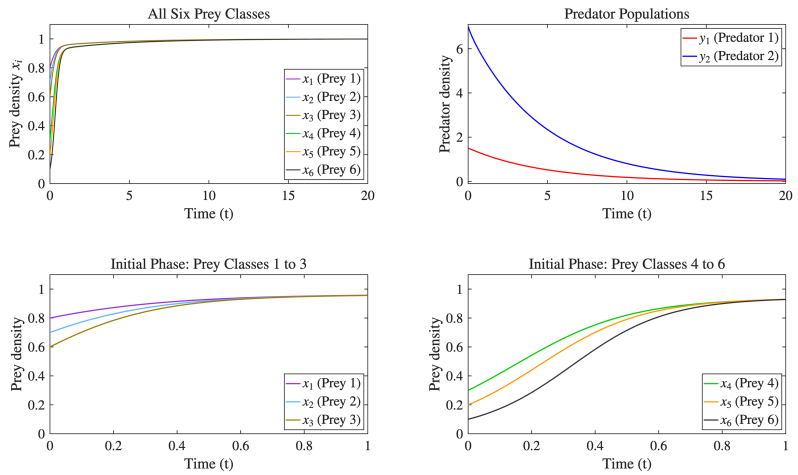


(a) Scenario N1

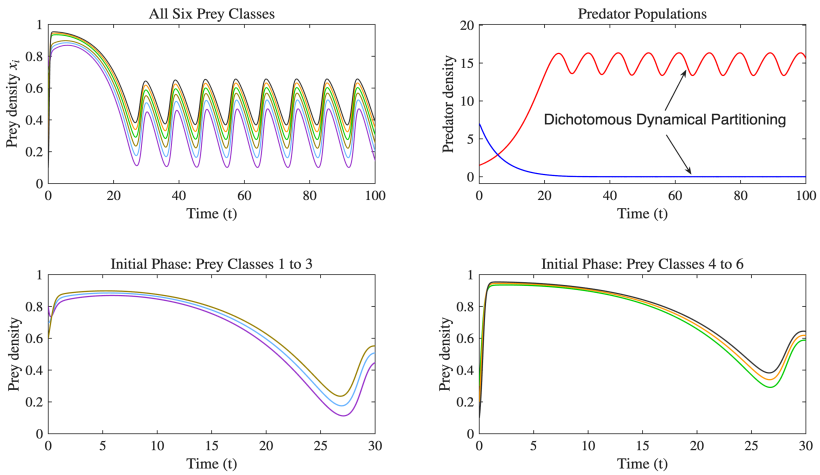


(b) Scenario N2

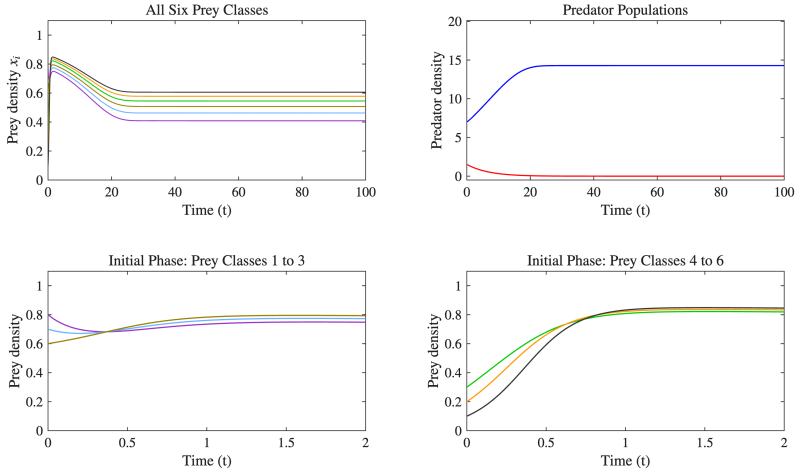


(c) Scenario N3

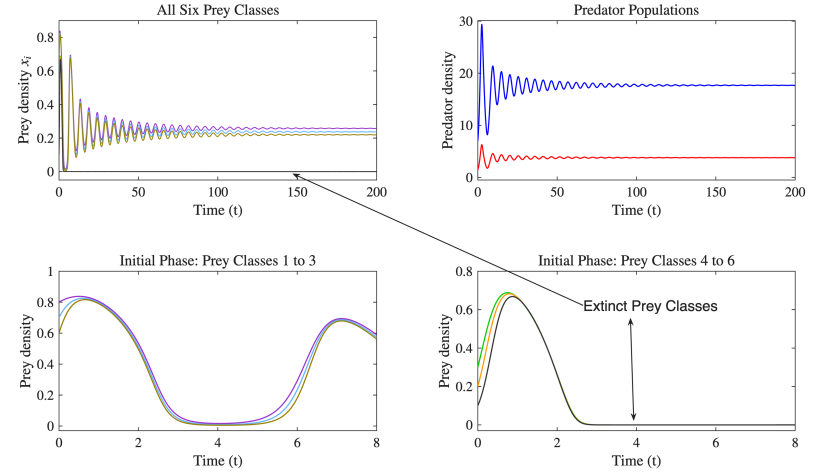


(d) Scenario N4

**Figure 4.** Summary of the four dynamical regimes for the two-predator, six-prey system based on the ecological reproduction numbers $R_{01}$ and $R_{02}$: (a) Scenario N1, both predators are extinct ($R_{01} < 1,\ R_{02} < 1$); (b) Scenario N2, predator 1 is extinct, whereas predator 2 persists ($R_{01} < 1,\ R_{02} > 1$); (c) Scenario N3, predator 2 is extinct, whereas predator 1 persists ($R_{01} > 1,\ R_{02} < 1$); and (d) Scenario N4, both predators persist ($R_{01} > 1,\ R_{02} > 1$).

**Table 6.** Summary of the dynamical scenarios explored in Figure 2.

| Scenario | Perspective | Observed behavior |
|---|---|---|
| **I1** | Predator 1 population | Goes extinct ($y_1(t) \to 0$). |
| | Predator 2 population | Goes extinct ($y_2(t) \to 0$). |
| | Prey populations | All prey approach their carrying capacities ($x_i(t) \to 1$, $i = 1, \ldots, 6$). |
| | Stability of the predator-free equilibrium $E_f$ | Locally asymptotically stable. |
| | Type of dynamics | Steady behavior. |
| **I2** | Predator populations | Persist at the single-predator equilibrium $E_Y^*$, where the total predator biomass satisfies $Y^* > 0$. |
| | Prey populations | Reach new equilibrium values; $x_i(t) \to x_i^* < 1$ for the preferred prey (1–3) consumed by $Y^*$. |
| | Stability of the single-predator equilibrium $E_Y^*$ | Saddle; predator 1 invades. |
| | Type of dynamics | Steady behavior. |
| **I3** | Predator populations | Persist at the single-predator equilibrium $E_Y^*$, where the total predator biomass satisfies $Y^* > 0$. |
| | Prey populations | Reach new equilibrium values; $x_i(t) \to x_i^* < 1$ for the preferred prey (4–6) consumed by $Y^*$. |
| | Stability of the single-predator equilibrium $E_Y^*$ | Saddle; predator 2 invades. |
| | Type of dynamics | Steady behavior. |
| **I4** | Predator 1 population | Persists with oscillatory dynamics; $y_1(t)$ fluctuates periodically. |
| | Predator 2 population | Persists with oscillatory dynamics; $y_2(t)$ fluctuates periodically. |
| | Prey populations | Exhibit oscillatory behavior around the coexistence-continuum equilibrium $\mathcal{E}$. |
| | Stability of the predator-free equilibrium $E_f$ | Unstable; both predators invade. |
| | Type of dynamics | Oscillatory (periodic) behavior. |

6.3.1. When the predators have identical behaviors

Figure 5 informs that the two predators undergo dynamic changes in all four examined scenarios, where the variations of the death rates regulate their dynamic behaviors. For example, if we fix the death rate of predator 1 ($\delta_1$) at 0.9 in scenario I1 and we increase $\delta_2$, then there is a dynamic change in the behavior of the system's dynamic, where the system moves from the blue regime to the red regime.

Also, Figure 5 tells that all other scenarios contain a variety of dynamical regimes depending on the values of the death rates $\delta_1$ and $\delta_2$. However, we can clearly see that scenario I4 has only three regimes where there is a compete absence of the green region. Plus, the coexistence of the two predators is conditional on the linear increase in their death rates, as depicted by the yellow line-like region.

It is worth pointing out that scenario I1 and scenario I2 take the same sizes of regions, which means that the two predators have the same tendency to the classes of prey. We mathematically distribute this to the existence of stability of the single-predator equilibrium $E_Y^*$, where $Y^*$ biologically represents the total biomass of the two predators as already described in Table 6.

6.3.2. When the predators have non-identical behaviors

Figure 6 exhibits that the two predators show distinct dynamical changes across all four examined scenarios, with variations in their death rates controlling the non-identical predator system's behavior. For example, when the death rate of predator 1, $\delta_1$, is fixed at 0.32 in scenario N1 and the death rate of predator 2, $\delta_2$, is increased slightly from 0.1 to 0.4, the system undergoes four successive dynamical transitions: blue, yellow, blue again, and finally red.

It is also shown in Figure 6 that the other scenarios display a variety of regimes depending on the values of $\delta_1$ and $\delta_2$. However, the green and red regions obviously dominate the overall dynamical landscape unless both death rates are extremely low.

It is noteworthy that the sizes of the regions vary significantly across the four scenarios, indicating that there is little overlap in the two predators' intake across the prey classes. As previously mentioned in Table 7, this depicts that the two predators feed on different prey classes mathematically, reflecting the existence of attractors.

To end this section, it is worth mentioning that model (3.1) does not include time delays. Although there may be significant delays between consuming prey and producing new predators, or between prey birth and their availability to predators, incorporating time delays would introduce infinite-dimensional dynamics and complicate the stability analysis considerably. Also, the novel model (3.1) is obviously deterministic and does not account for any stochasticity. These simplifications help in studying standard techniques of local and global stability analysis. Although incorporating time delays and stochasticity are still important for understanding extinction risk even in small populations, our focus here is restricted to the deterministic conditions for coexistence and persistence.

## 7. Ecological interpretation of parameter selection

In this section, we give a thorough ecological rationale for our numerical simulations and the parameter selections shown in Tables 4 and 5. In other words, the parameter sets are intentionally selected to explore a spectrum of ecological scenarios. To be more specific, we consider contrasting foraging strategies (generalist versus specialist predators), varying levels of predation efficiency, and

prey of different nutritional quality. Therefore, these choices answer some fundamental ecological questions regarding predator coexistence, interspecific competition, and the stability of multi-prey communities. Furthermore, the parameter ranges are tailored to give a wide spectrum of ecological reproduction numbers $R_0$, with different values. This definitely allows us to examine the conditions under which the predator populations persist or go extinct in symmetric and asymmetric cases.

### *7.1. Ecological rationale for scenarios of the identical predators*

In Table 4, both predators are assumed to have identical parameter sets (i.e., $p_{i1} = p_{i2} = p_i$, $b_{i1} = b_{i2} = b_i$, $c_{i1} = c_{i2} = c_i$). This represents the case two predator species have identical foraging capabilities. As a result, we have offered four scenarios exploring different ecological strategies.

In scenario I1 (low efficiency generalists), the parameter values ($p_i = 0.25$ for all prey, $b_i = 0.50$, $c_i = 0.25$) are selected to depict a predator that exhibits low conversion efficiency ($c_i$), consumes moderate handling times ($b_i$), and is inefficient at capturing prey ($p_i = 0.25$). It is a poor forager on nutritionally deficient prey, such as an ambush predator that has poor success rates while hunting low-quality or well-defended prey. The community of relatively fast-reproducing species, such as insects or small animals, is represented by the moderate prey growth rates ($a_i = 5.0 - 7.5$). This scenario, with $R_0 = 0.431$, depicts a habitat where predators exist but are unable to sustain a viable population in the absence of immigration. From an ecological perspective, this scenario shows how predators can persist in an ecosystem without being able to support themselves.

In scenario I2 (predatory specialists (prefer prey 1–3)), lower attack rates on prey 4–6 ($p_i = 0.25, 0.20, 0.15$) and high attack rates on prey 1–3 ($p_i = 0.70, 0.65, 0.60$), suggesting morphological or behavioral specialization for capturing specific prey species. A predator that specializes in small animals is an example of a traditional "dietary specialist". The handling times are uniformly low ($b_i = 0.25$ for all prey), informing that once captured, consumption is fast regardless of the prey type. However, the conversion efficiency is high for some preferred prey ($c_i = 0.75$) and low for the non-preferred prey ($c_i = 0.25$), reflecting the nutritional superiority of the preferred prey. With the basic reproduction number $R_0 = 1.5 > 1$, the predator can clearly persist by specializing on prey 1–3. The high values of PFI (1.95–2.10) for prey 1–3 quantify this preference. This scenario demonstrates the benefits and risks of dietary specialization.

Scenario I3 (predatory specialists (prefer prey 4–6)) is the mirror image of scenario I2, with the predator preferring prey 4–6 ($p_i = 0.60, 0.65, 0.70$) over the first three classes of prey 1–3 ($p_i = 0.15, 0.20, 0.25$). This is an example of a predator that preys on slower-growing but more nutritious prey. The greater $R_0 = 2.5 > 1$ in comparison to I2 indicates that these prey are often more profitable. This situation shows how a predator can effectively take advantage of a distinct subgroup of the prey community and that it may be more beneficial to specialize on more nutritious prey than on quickly growing but less nutritious prey.

Scenario I4 (high efficiency generalists) mimics a highly successful generalist predator with maximum attack rates ($p_i = 1.00$ for all prey), very low handling times ($b_i = 0.25$), and very high conversion efficiency ($c_i = 0.90$). Such selected values characterize the predator that is highly efficient in capture and consumption of prey, like those with advanced sensory capabilities. With $R_0 = 2.7 > 1$, the predator exerts strong top-down control on the prey community. Thus, this scenario can serve as a baseline for understanding maximum predator efficiency and its consequences for community dynamics.

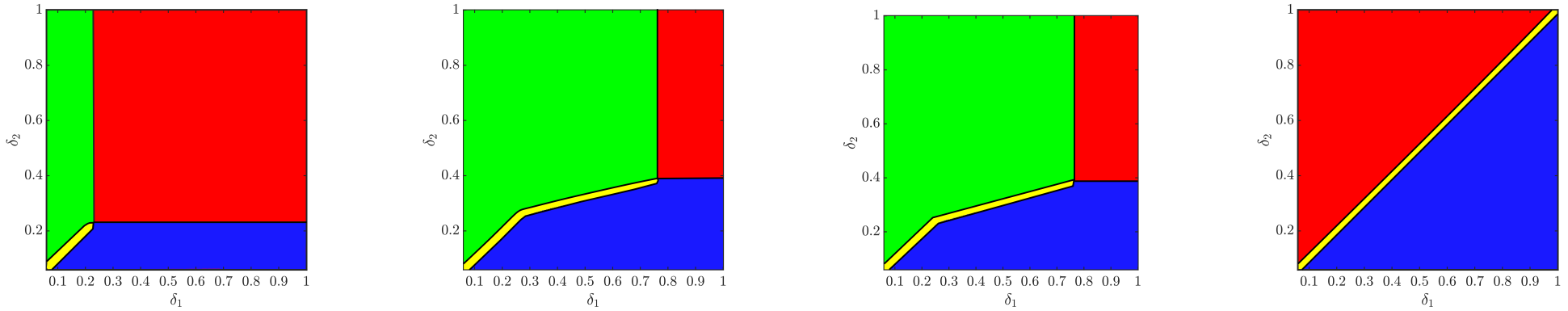


(a) Scenario I1 (b) Scenario I2 (c) Scenario I3 (d) Scenario I4

**Figure 5.** Effect of variations in the death rates of two predators with identical feeding behaviors, using the parameter values listed in Table 4.

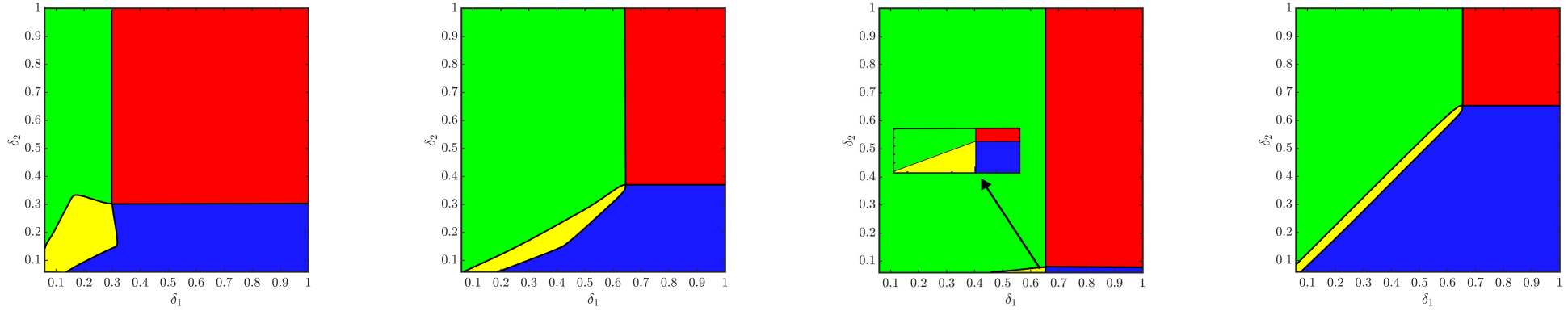


(a) Scenario N1 (b) Scenario N2 (c) Scenario N3 (d) Scenario N4

**Figure 6.** Effect of variations in the death rates of the two predators with non-identical feeding behaviors, using the same parameter values stated in Table 5.

**Table 7.** Summary of the dynamical scenarios explored in Figure 4.

| Scenario | Perspective | Observed behavior |
|---|---|---|
| **N1** | Predator 1 population | Goes extinct ($y_1(t) \to 0$). |
| | Predator 2 population | Goes extinct ($y_2(t) \to 0$). |
| | Prey populations | All prey approach their carrying capacities ($x_i(t) \to 1$, $i = 1, \ldots, 6$). |
| | Stability of the complete predator-free equilibrium $E_f$ | Locally asymptotically stable. |
| | Type of dynamics | Steady behavior. |
| **N2** | Predator populations | Persist at the predator-1 equilibrium $E_1^*$; only predator 1 coexists ($y_1(t) > 0$). |
| | Prey populations | Persist with oscillatory dynamics; $x_i(t) \to x_i^* < 1$ and fluctuate periodically. |
| | Stability of the predator-1 persistence equilibrium $E_1^*$ | Saddle; predator 1 invades. |
| | Type of dynamics | Oscillatory (periodic) behavior. |
| **N3** | Predator populations | Persist at the predator-2 equilibrium $E_2^*$; only predator 2 coexists ($y_2(t) > 0$). |
| | Prey populations | Persist with stable dynamics; $x_i(t) \to x_i^* < 1$. |
| | Stability of the predator-2 persistence equilibrium $E_2^*$ | Saddle; predator 2 invades. |
| | Type of dynamics | Steady behavior. |
| **N4** | Predator 1 population | Persists with stable dynamics; $y_1(t)$ approaches a steady state. |
| | Predator 2 population | Persists with stable dynamics; $y_2(t)$ approaches a steady state. |
| | Prey populations | Persist with stable dynamics; $x_i(t) \to x_i^* < 1$. |
| | Stability of the coexistence equilibrium $E^*$ | Globally asymptotically stable. |
| | Type of dynamics | Steady behavior. |

### 7.2. Ecological rationale for scenarios of the non-identical predators

In Table 5, the two predators have four separate parameter sets ($p_{i1} \neq p_{i2}$, $b_{i1} \neq b_{i2}$, $c_{i1} \neq c_{i2}$), indicating two different predator species with differing body sizes, food preferences, or foraging strategies. This enables us to investigate competition and niche differentiation.

In scenario N1 (complete niche partitioning), predator 1 specializes on prey 1–3 (high $p_i$, moderate $b_i$, high $c_i$) while predator 2 specializes on prey 4–6 (high $p_i$, moderate $b_i$, high $c_i$). The values of the PFI confirm this complete niche separation: the PFI for predator 1 on prey 1–3 is high (0.90–0.98), while the PFI for predator 2 on prey 4–6 is equally high. This is resource partitioning, a mechanism observed in nature to reduce competition between several coexisting species. Interestingly, despite this niche partitioning, each predator individually has $R_0 < 1$, suggesting that neither predator can sustain its population alone on its preferred prey alone. This asserts the importance of dietary flexibility for predator persistence and suggests that complete specialization may be a risky strategy.

In scenario N2 (generalist versus specialist), predator 1 is a generalist with high attack rates ($p_i = 0.90$), low handling times ($b_i = 0.30$), and high conversion efficiency ($c_i = 0.80$) on all prey. Predator 2 is a specialist on prey 1–3 with high $p_i$, moderate $b_i$, and high $c_i$, but low efficiency on prey 4–6. The reproduction numbers are given by $R_0^{(1)} = 1.263 > 1$ and $R_0^{(2)} = 0.71 < 1$, which indicate that the generalist predator can persist while the specialist cannot. An ecosystem where a generalist predator (like a coyote) outcompetes or coexists with a specialist predator (like a lynx that specializes in rabbits) is rationally explained by this scenario.

Scenario N3 (specialist versus generalist) is the reverse of scenario N2, with predator 1 as the specialist and predator 2 as the generalist. The reproduction numbers here are given by $R_0^{(1)} = 0.74 < 1$ and $R_0^{(2)} = 1.15 > 1$, showing that the generalist again has the advantage. Comparing N2 and N3 allows us to examine how the relative strengths of specialization and generalization influence coexistence.

In scenario N4 (cross specialization), both predators are highly efficient specialists with very high conversion efficiency ($c_i = 1.00$ for all prey). Predator 1 prefers prey 1–3, while predator 2 prefers prey 4–6. With $R_0^{(1)} = R_0^{(2)} = 2.61 > 1$, both predators can persist independently. This mimics the overlapping but different prey preferences of two extremely effective top predators in the same ecosystem, such as lions and hyenas. The high reproduction number $R_0$ values inform that both predators can coexist, but their interaction may lead to intense competition depending on the predators' mortality rate $\delta_j$.

### 7.3. Ecological motivation for numerical simulations

We can say that the presented numerical simulations address four key ecological questions. First, we examine whether resource differentiation alone is sufficient for predator coexistence or whether factors like conversion efficiency are more important by contrasting scenarios of complete niche partitioning (N1) and cross specialization (N4). Second, although a moderate level of exploitive competition ($\delta_j = 0.50$) is assumed in every scenario, this establishes a baseline for further investigation into how different temporal interference influences community structure through intraguild predation and competition. Third, we assess the correlation between the ecological reproduction number and ecosystem stability by comparing scenarios with $R_0 < 1$ (e.g., I1, N1) versus $R_0 > 1$ (e.g., I4, N4), testing whether greater $R_0$ encourages stable predator-prey cycles or instead drives prey to extinction. Fourth, we may assess whether generalist predators are more resilient to prey changes by contrasting generalist and

specialist strategies (scenarios N2 and N3). This is a crucial question given climate change and habitat fragmentation. These simulation scenarios collectively provide a comprehensive framework for understanding the ecological mechanisms that govern predator coexistence and community stability in multi-prey ecosystems.

### *7.4. Ecological implications of global stability, specialization, and the preference index*

It is theoretically discussed that the global stability results, established earlier, undoubtedly tell profound ecological implications for understanding long-term dynamics that show the persistence of the populations. When the coexistence equilibrium is globally asymptotically stable under certain conditions, this implies that, regardless of the initial population densities, our model will inevitably converge to a coexisting state where all prey and predator populations persist while none of the predator populations goes extinct. For example, scenario I4 in Figure 2 confirms the result of global stability numerically in model (5.4), where all the classes of prey and two predator populations persist in an oscillatory pattern around the coexistence equilibrium $\mathcal{E}$.

We also can observe that specialization plays a critical role in predator survival. This is obvious in some of our found results. For instance, generalist predators tend to have higher values of $R_0^{(1)}$ than specialists $R_0^{(2)}$ in scenario N2 (see Table 5). The generalist predator (predator 1) has $R_0^{(1)} = 1.263$, while the specialist predator (predator 2) has $R_0^{(2)} = 0.71$. This suggests that nutritional diversity acts as protection against changes in prey, strengthening generalist strategies in variable environments. However, generalists may not be as efficient at capturing any single prey class as a specialist would be.

The PFI is biologically useful because it allows us to predict which prey species a predator is most likely to select. Prey with higher PFI values are more profitable and should be preferred by the predator. Also, the PFI can be used to quantify niche differentiation between predators. When two predators have high PFI values for different prey species (as observed in scenario N2), this indicates resource partitioning, which can facilitate coexistence by reducing competition. Also, when both predators have opposite PFI values for the prey classes (as noticed in scenario N4), this indicates the existence of cyclic oscillations.

## 8. Conclusions

The analysis presented in this paper provides a foundation for understanding more complex two-predator, multi-prey models. Here, the presented framework has been extended to incorporate a variety of interactions in an ecosystem with two predators exhibiting different feeding behaviors across multiple prey classes. To be more specific, we extended the Holling type-II functional response to model the interaction dynamics of two predator species consuming distinct classes of prey. This extension represents a significant step beyond the single-predator model, as it captures the added complexity of interspecific competition between the two predators and the possibility of either coexistence or competitive exclusion.

In order to guarantee that all solutions continue to be globally well-behaved and biologically significant, we formulated exact results based on positivity and boundedness. Under symmetric and asymmetric predator-prey interactions, analytical expressions for the equilibrium points were obtained, and appropriate Lyapunov functions were used to demonstrate the global stability of the coexistence equilibria in both scenarios. All analytical results were validated by numerical simulations, which also

demonstrated a wide range of dynamical behaviors in each of the four different scenarios. In order to better integrate the model with real-world populations, future research should study spatial extensions, stochastic effects, and data-driven parameterization. Also, one can consider potential bifurcations for the two cases where there is clear evidence of the emergence of several types of bifurcations, such as Hopf, pitchfork, and fold. These results highlight how important predator specialization and interaction structure are in shaping ecosystem dynamics.

The explored results of this study interestingly provide several important ecological insights that go beyond the mathematical analysis. For example, the found ecological reproduction number $R_0$ emerges as a critical threshold parameter that determines whether the two predator populations can persist in a multi-prey community. When $R_0 < 1$, the predators cannot sustain and will eventually go extinct regardless of the initial population densities. This finding directly affects conservation biology since it implies that even in scenarios in which prey appear abundant, predator populations may be at risk of extinction if the prey are difficult to hunt. Conversely, when $R_0 > 1$, the predators can persist, but the equilibrium values depend on several factors such as prey growth rates, attack rates, handling times, and conversion efficiencies.

Also, our numerical simulations with two predator species (Table 5) inform that predator coexistence can be facilitated by niche differentiation, but only under certain conditions. When the predators have high conversion efficiencies (scenario N4: cross specialization), they can coexist even if overlapping prey preferences occurs. However, when one predator is a specialist and the other generalist (scenarios N2 and N3), the latter tends to have a higher reproduction number and may competitively exclude the former. This finding has significant consequences for understanding how predator groups form and persist in natural ecosystems. For instance, large carnivores, such as lions, spotted hyenas, and leopards, exhibit varying degrees of dietary specialization and generalism in African savannas [15, 16]. In our model, this suggests that the coexistence of such predators may depend on some differences in their prey preferences and foraging efficiencies.

In a nutshell, we here provided an analytical and numerical framework for understanding the rich dynamics of multi-prey, two-predator models, and it opens avenues for further investigations into deeper ecological interactions and control strategies for the interested researchers.

## Author contributions

Hanan Saeed developed the statistically conceptual framework and carried out all statistical analyzes. Nouf A. Alrubea and Mehmet Yavuz jointly revised the model formulation and contributed the analytical components of the study. Ali Sarrah developed the conceptual framework, mathematically formulated and numerically implemented the full model, and interpreted and described all the resulting dynamical behaviors. All authors have read and approved the final manuscript.

## Use of Generative-AI tools declaration

The authors declare they have not used Artificial Intelligence (AI) tools in the creation of this article.

## Conflict of interest

The authors declare that they have no conflicts of interest.

## References


1. A. Sarrah, F. J. Alanazi, M. Yavuz, S. Saber, The effects of fluctuating carrying capacity on the dynamics of a Holling-type III predator-prey model, *J. Math.*, **2026** (2026), 5067259. https://doi.org/10.1155/jom/5067259
2. F. M. K. Almalki, E. Solouma, M. Yavuz, S. Saber, A. Sarrah, Analytical and numerical study of bifurcations and reaction-diffusion patterns in a predator-prey model with Holling III response and variable carrying capacity, *Ain Shams Eng. J.*, **17** (2026), 104131. https://doi.org/10.1016/j.asej.2026.104131
3. F. M. K. Almalki, G. Alhamzi, M. Bin-Asfour, E. Solouma, N. Almutairi, A. Sarrah, et al., Ecological and epidemiological thresholds in a predator-prey system with cross-infection: stability, bifurcations, and reaction-diffusion dynamics, *AIMS Math.*, **11** (2026), 7695–7739. https://doi.org/10.3934/math.2026317
4. X. Y. Meng, N. N. Qin, H. F. Huo, Dynamics analysis of a predator-prey system with harvesting prey and disease in prey species, *J. Biol. Dyn.*, **12** (2018), 342–374. https://doi.org/10.1080/17513758.2018.1454515
5. P. Kumar, S. Raj, Modelling and analysis of prey-predator model involving predation of mature prey using delay differential equations, *Numer. Algebra Control Optim.*, **12** (2022), 783–791. https://doi.org/10.3934/naco.2021035
6. E. van Leeuwen, Å. Brännström, V. A. A. Jansen, U. Dieckmann, A. G. Rossberg, A generalized functional response for predators that switch between multiple prey species, *J. Theor. Biol.*, **328** (2013), 89–98. https://doi.org/10.1016/j.jtbi.2013.02.003
7. T. K. Kar, Stability analysis of a prey-predator model incorporating a prey refuge, *Commun. Nonlinear Sci. Numer. Simul.*, **10** (2005), 681–691. https://doi.org/10.1016/j.cnsns.2003.08.006
8. C. S. Holling, Some characteristics of simple types of predation and parasitism. *Can. Entomol.*, **91** (1959), 385–398. https://doi.org/10.4039/Ent91385-7
9. H. Molla, M. S. Rahman, S. Sarwardi, Dynamics of a predator-prey model with Holling type-II functional response incorporating a prey refuge depending on both the species, *Int. J. Nonlinear Sci. Numer. Simul.*, **20** (2019), 89–104. https://doi.org/10.1515/ijnsns-2017-0224
10. S. Fatah, A. Mustafa, S. Amin, Predator and n-classes-of-prey model incorporating extended Holling type-II functional response for n different prey species, *AIMS Math.*, **8** (2023), 5779–5788. https://doi.org/10.3934/math.2023291
11. M. W. Hayward, G. I. H. Kerley, Prey preferences of the lion (Panthera leo), *J. Zoology*, **267** (2005), 309–322. https://doi.org/10.1017/S0952836905007508
12. J. M. Jeschke, M. Kopp, R. Tollrian, Predator functional responses: discriminating between handling and digesting prey, *Ecology*, **72** (2002), 95–112. https://doi.org/10.1890/0012-9615(2002)072[0095:PFRDBH]2.0.CO;2

13. M. Kot, *Elements of mathematical ecology*, Cambridge University Press, 2001.

14. G. T. Skalski, J. F. Gilliam, Functional responses with predator interference: viable alternatives to the Holling type-II model, *Ecology*, **82** (2001), 3083–3092. https://doi.org/10.1890/0012-9658(2001)082[3083:FRWPIV]2.0.CO;2

15. C. Packer, D. Scheel, A. E. Pusey, Why lions form groups: Food is not enough, *Amer. Nat.*, **136** (1990), 1–19. https://doi.org/10.1086/285079

16. H. E. Watts, K. E. Holekamp, Ecological determinants of survival and reproduction in the spotted hyena, *J. Mammalogy*, **90** (2009), 461–471. https://doi.org/10.1644/08-MAMM-A-136.1




AIMS Press

© 2026 the Author(s), licensee AIMS Press. This is an open access article distributed under the terms of the Creative Commons Attribution License (https://creativecommons.org/licenses/by/4.0)